DAMPING AND DISPERSION OF TWISTED-PAIR TRANSMISSION LINE AND A COMPENSATION METHOD TO IMPROVE LOCATION OF IMPEDANCE DISCONTINUITIES

by

Rebecca W. Ross

Submitted to the Graduate Faculty of

the Swanson School of Engineering in partial fulfillment

of the requirements for the degree of

Master of Science

University of Pittsburgh

2008

UNIVERSITY OF PITTSBURGH

SWANSON SCHOOL OF ENGINEERING

This thesis was presented

by

Rebecca W. Ross

It was defended on

November 21, 2008

Thesis Advisor: Dr. Patrick Loughlin, PhD, Professor

Dr. Amro El-Jaroudi, PhD, Associate Professor

Dr. Mahmoud El Nokali, PhD, Associate Professor

DAMPING AND DISPERSION OF TWISTED-PAIR TRANSMISSION LINE AND A COMPENSATION METHOD TO IMPROVE LOCATION OF IMPEDANCE DISCONTINUITIES

Rebecca W. Ross, M.S.

University of Pittsburgh, 2008

In this thesis, a method to compensate for propagation effects in twisted-pair transmission lines is developed, with a goal of improving the location of impedance discontinuities in the line. There are many methods to locate impedance discontinuities, among them are single-ended measurements using frequency domain reflectometry (FDR), which is the focus of this work. With FDR, one transmits a steady-state tone or tones onto the line, then measures the amplitude and phase difference of the tone at the receiver relative to the transmit tone. Propagation effects of the line, especially damping and dispersion, which are generally unknown, can negatively impact the performance of FDR methods, making identification of impedance discontinuities difficult.

A method is presented to compensate for the damping without requiring a priori knowledge of the cable type and length. In the absence of impedance mismatches between the source and the line, the compensation method improves impedance discontinuity location. Performance of the method degrades considerably when there is an impedance mismatch, but a procedure to compensation for this effect is presented. This compensation requires an assumption of the initial cable type and impedance of test equipment's connecting path. Results are presented on simulations and field data to quantify the performance of the method and identify benefits and limitations.

TABLE OF CONTENTS

LIST OF TABLES

LIST OF FIGURES

1.0 BACKGROUND

1.1 TWISTED-PAIR

Lines (or loops) typically used in telephony are 1kft to 25kft twisted pair cable [2]. These loops can be a variety of cable types and gauges and are connected to the customer via a single twisted pair from a central office location. Central offices contain equipment to drive and test the telephone lines and provide connection to other offices. Figure 1 shows a simplified diagram of this connection. For the best service to the customer the impedance of the loop should be continuous and matched well with the customer termination for the frequencies transmitted. This is especially the case for higher frequency services such as xDSL [4].

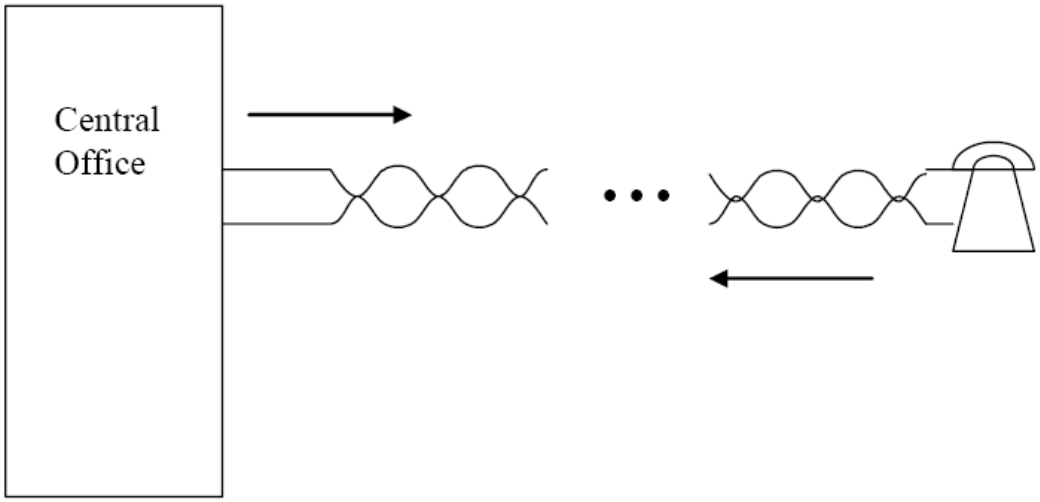

Figure 1: Simplified block diagram of typical telephone line service

When there is an impedance discontinuity some of the transmitted energy is reflected back to the sender thus reducing the energy that continues on to the receiver. Frequency domain reflectometry (FDR) is a method of gaining information about a twisted-pair transmission line, which can be used to determine the location of these discontinuities [6]. Another method of finding impedance discontinuities is time-domain reflectometry (TDR) [6]. Both methods are single ended measurements, meaning the test equipment is located only in the central office taking advantage of being able to test many lines with one piece of equipment without needing someone or special equipment at the customer site. However, an advantage of FDR over TDR is the amount of energy sent into the system is spread out over time and thus can be easier to implement and calibrate with hardware circuitry [3]. FDR can be measured many ways [3] [4]. One way is to send a tone connected to the line under test (LUT) and measure the amplitude and phase difference at the LUT from what was sent. This FDR value per frequency is complex with magnitude less than one.

Impedance characteristics of twisted pair cable have been studied and measured extensively [1] [2]. Twisted pair cable has a distributed impedance, which can be modeled as a bulk entity with variable components dependent upon frequency, cable type and section length. In a two-port model sense, twisted pair cable can be modeled as [1] [2]:

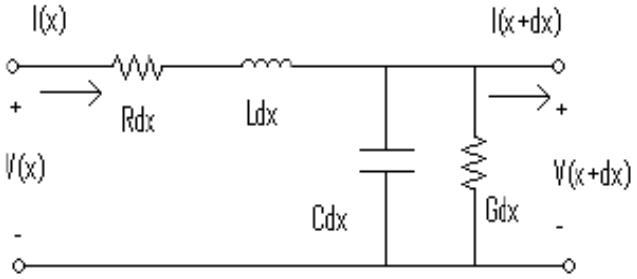

Figure 2: Two-port model of incremental section of twisted pair transmission line.

A transmission line can be viewed as a cascade of these incremental sections [1]. The capacitance is fixed by design, while the inductance (L), resistance (R) and conductance (G) are variable across frequency and conduction type. These variations are a result of conductor diameter and skin effects about the perimeter of the cable. There is also interaction

with other pairs within a cable bundle which effects the impedance. The more pairs within the bundle the more stable this interaction is. The voltage and current through this infinitesimally small two port model can be defined with two first-order differential equations [1],

$$\begin{aligned} -\frac{dV}{dx} &= (R(\omega) + j\omega L(\omega))\, I \\ -\frac{dI}{dx} &= (G(\omega) + j\omega C)\, V \end{aligned} \tag{1.1}$$

The solution to these differential equations is a frequency and cable dependent propagation constant $\gamma(\omega)$, where

$$\gamma(\omega) = \pm\sqrt{(R(\omega) + j\omega L(\omega))(G(\omega) + j\omega C)} \tag{1.2}$$

The propagation constant characterizes the positive and negative going waves whose sum is the total signal. These waves can be shown to vary by $e^{\pm\gamma(\omega)x}$ [1]. The propagation constant is complex with the real part, α, defining the damping part of the propagation and the imaginary part, β, defining the dispersion part of the propagation.

$$\gamma(\omega) = \alpha(\omega) + j\beta(\omega) \tag{1.3}$$

The damping and dispersion cause difficulty in finding impedance discontinuities because it distorts propagating pulses as shown in preliminary work described in the following Chapter 2.

2.0 PRELIMINARY WORK

2.1 FIELD TESTING

A common technique in finding impedance discontinuities is to propagate a pulse down a twisted pair cable and if there is an impedance discontinuity, part or all of the sent pulse will propagate back to the sender [6]. The time difference from the sent pulse to the returned pulse is proportional to the distance from the sent pulse start to the impedance discontinuity. However because of the line's damping and dispersion, finding returned pulses can be difficult. One method of finding information about a twisted pair cable is the FDR method described in Chapter 1. Figures 3 and 4 show the magnitude and phase of the FDR, respectively, for a field collected line with and without a fault or impedance discontinuity condition.

In the field data, there is a slight difference in the magnitude and phase of a line with and without a fault. More processing than just viewing the FDR magnitude and phase is needed to determine if and where a fault occurs. If we look at the impulse response of this frequency sweep we can locate the impedance mismatches better, as shown in Figure 5. However, we still have difficulty in finding locations further out because the damping and dispersion cause the pulse to be distorted. Figures 6, 7, and 8 illustrate this distortion.

Figures 6, 7, and 8 are the time domain plots of a time domain impulse applied to the FDR data collected in a lab. The time x-axis is scaled to distance using a nominal propagation constant. The time domain impulse was applied by multiplying a low pass filter to the FDR data and calculating the iFFT then plotting the real part only. This operation simulates a TDR (simulated TDR). Comparing plots 6 and 7, the impulse widens and drops significantly in amplitude. However in Figure 8, the impulse becomes very distorted and loses even more amplitude. Figure 9 shows a zoomed in view of the reflection associated with the

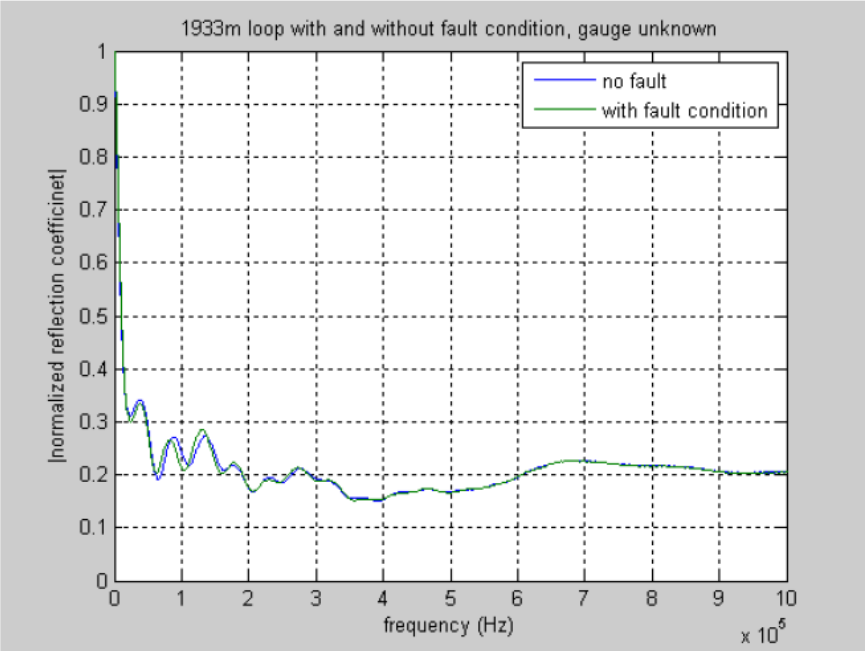

Figure 3: Magnitude of twisted pair with/without fault condition, field collected

end-of-line. At 15kft the reflection is quite distorted from the original signal which causes problems for many processing techniques including correlation. Taking a difference may be able to draw out the impulse in this particular case, however simply taking a difference would also draw out all changes in slope some of which are not important in characterizing the line. Also note in Figure 6 there is a second reflection associated with the end-of-line. This is because the receiver is not matched to the line impedance.

2.2 DAMPING AND DISPERSION

The distortion observed in the field data shown in Figures 6, 7, and 8 is the result of the damping and dispersion discussed in Chapter 1. Equations 1.2 and 1.3 describe the damping and dispersion of twisted pair cable. To understand the damping and dispersion of twisted

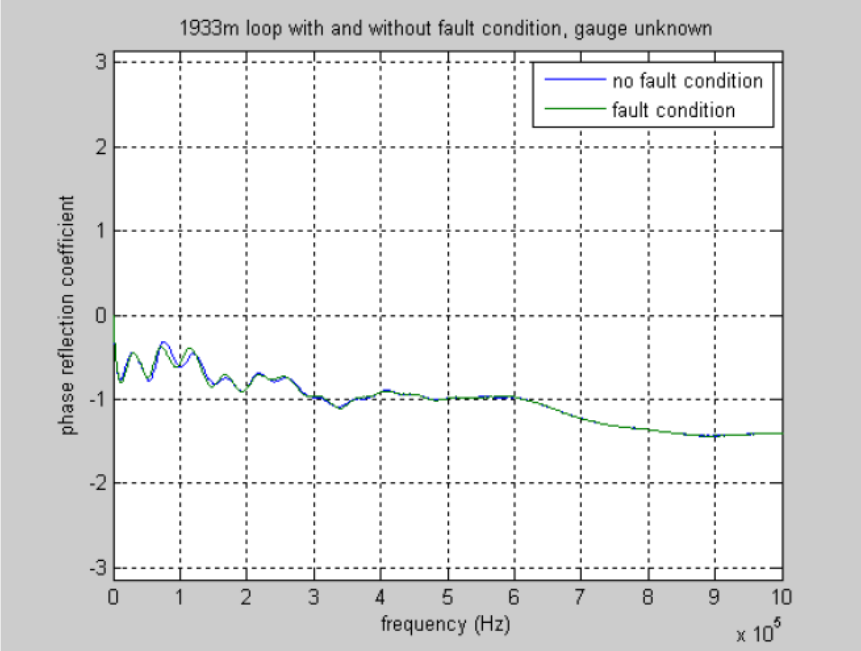

Figure 4: Phase of twisted pair with/without fault condition, field collected

pair cable, we need to expand equation 1.2 further, as follows:

$$\gamma(\omega) = \sqrt{(R(\omega)G(\omega) - \omega^2 L(\omega)C) + j\omega(L(\omega)G(\omega) + R(\omega)C)} \tag{2.1}$$

For the rest of this section, the frequency dependencies on R,G, and L will be dropped for ease of notation. If we define $a = (RG - \omega^2 LC)$ and $b = \omega(LG + RC)$, then

$$\gamma = \alpha + j\beta = \sqrt{a + jb} \tag{2.2}$$

and,

$$\gamma^2 = a + jb = (\alpha + j\beta)^2 = \left(\alpha^2 - \beta^2\right) + j(2\alpha\beta) \tag{2.3}$$

We can equate $a = \alpha^2 - \beta^2$ and $b = 2\alpha\beta$. Also, evaluating the magnitude squared of γ, we have:

$$|\gamma|^2 = \alpha^2 + \beta^2 = |a + jb| = \sqrt{a^2 + b^2} \tag{2.4}$$

with,

$$\alpha^2 + \beta^2 = \sqrt{a^2 + b^2} \tag{2.5}$$

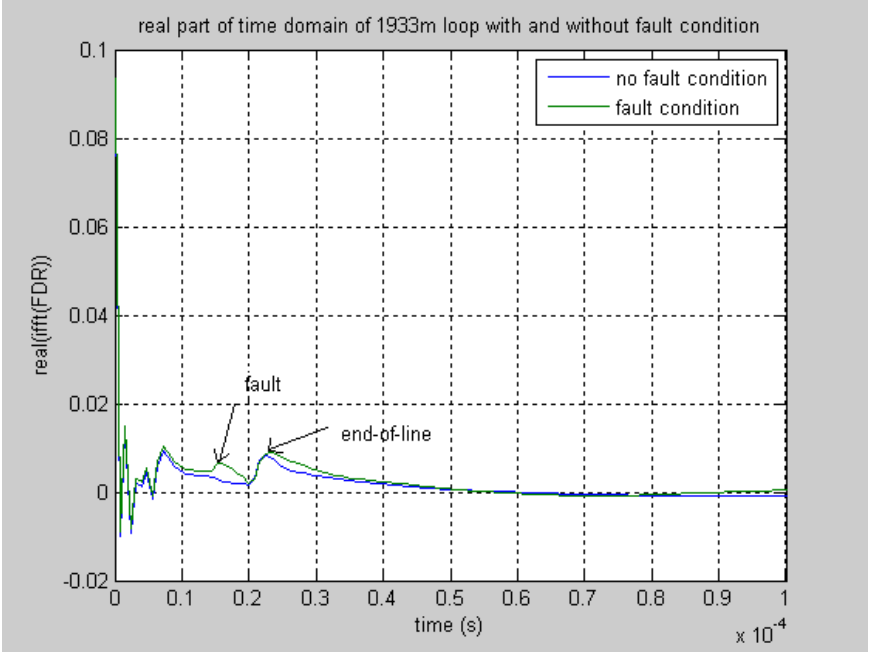

Figure 5: Real part of IFFT of FDR shown in Figures 3 and 4

and from equation 2.3, $\alpha^2 - \beta^2 = a$.

If we combine equations 2.4 and 2.5 we have:

$$2\beta^2 = \alpha^2 + \beta^2 - \left(\alpha^2 - \beta^2\right) = \sqrt{a^2 + b^2} - a \tag{2.6}$$

from which we can solve for β as:

$$\beta = \sqrt{\frac{1}{2}\left(\sqrt{a^2 + b^2} - a\right)} \tag{2.7}$$

For typical North American twisted pair cable, 22, 24, and 26 gauge PIC cable at 70 F^0, the values of R, L, G, and C for frequencies in the 1kHz to 1MHz range allow the term $a^2 + b^2$ to be simplified. Resistance, R, ranges $174 - 957\Omega/mile$, inductance, L, ranges $0.7950 - 0.9858mH/mile$, conductance, G, ranges $0.076 - 71.014\mu Mho/mile$, and capacitance, C, is $0.083\mu F/mile$ by design [2]. Expanding out $a^2 + b^2$ we have,

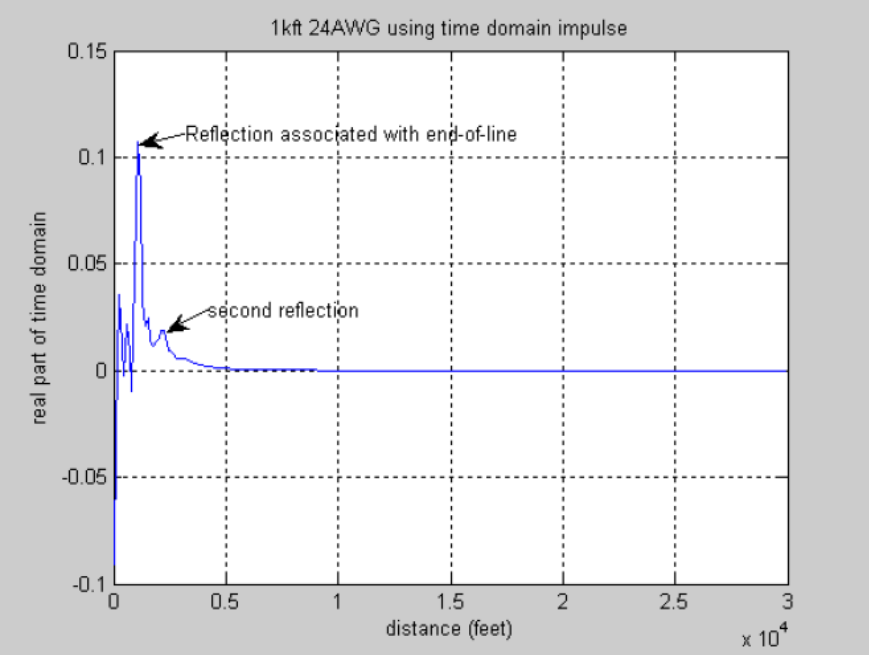

Figure 6: Impulse in time of 1kft line length (short line)

$$\begin{aligned} a^2 + b^2 &= \left(RG - \omega^2 LC\right)^2 + \left(\omega \left(LG + RC\right)\right)^2 \\ &= R^2 \left(G^2 + \omega^2 C^2\right) + \omega^2 L^2 \left(\omega^2 C^2 + G^2\right) \end{aligned} \tag{2.8}$$

$R^2 \left(G^2 + \omega^2 C^2\right)$ is very small in comparison to the second sum term $\omega^2 L^2 \left(\omega^2 C^2 + G^2\right)$ using the frequency range of 1kHz to 1MHz and typical North American twisted pair cable, additionally G^2 is much smaller than $\omega^2 C^2$, therefore:

$$a^2 + b^2 \simeq \omega^4 L^2 C^2 \tag{2.9}$$

and, $a = RG - \omega^2 LC$ can be approximated by:

$$a \simeq -\omega^2 LC \tag{2.10}$$

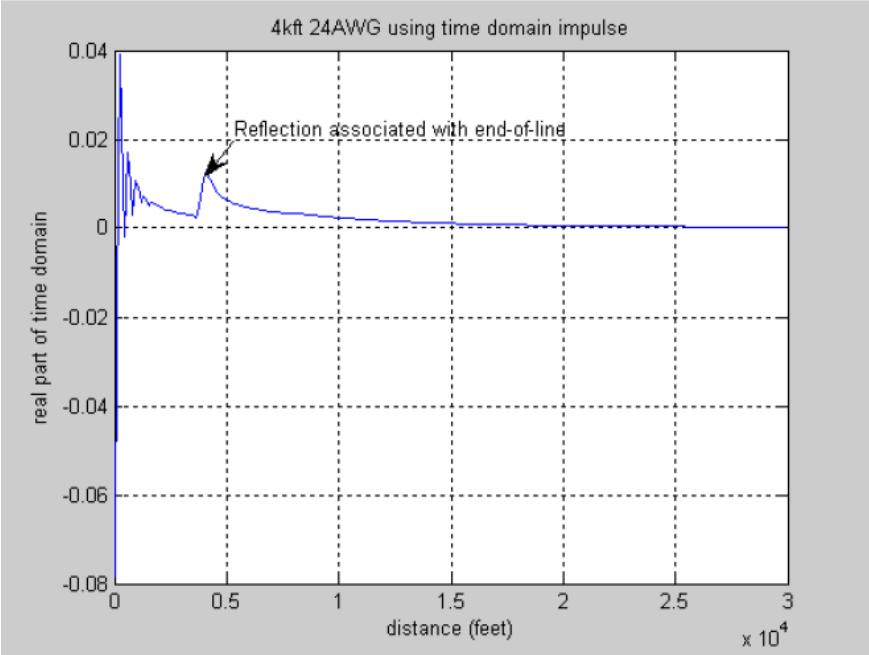

Figure 7: Impulse in time of 4kft line length (medium length line)

With those approximations and bringing frequency dependencies back in, β, can be approximated as:

$$\beta \simeq \omega\sqrt{L\left(\omega\right)C} \tag{2.11}$$

Note the frequency dependency of L prevents β from being linear with respect to ω. Dispersion is defined as the derivative of β with respect to ω. So this non-linearity causes frequency dispersion and is a direct a result of $L(\omega)$. If L was not frequency dependent then β' would be a constant and thus have no dispersion or all frequencies would travel at the same rate in the transmission line. However, in twisted pair transmission line L is frequency dependent and thus β' is frequency dependent such that low frequencies travel at a slower speed than high frequencies. See [6] for more information on the calculation of β and its derivative. Figure 10 shows a plot of $\frac{d\beta}{d\omega}$ over the frequency range 1kHz to 1MHz, which is the frequency range used for data collected in Figure 3.

The real part of the propagation α gives the damping portion or the loss expected for a

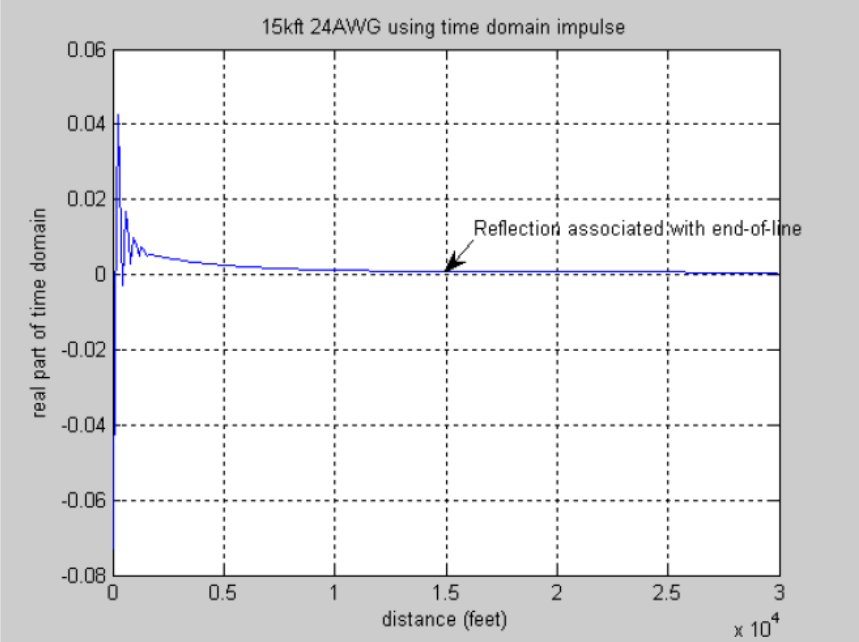

Figure 8: Impulse in time of 15kft line length (longer length line)

certain frequency. Using the above substitution, $b = 2\alpha\beta$, and solving for α and using the approximation of β we have:

$$\alpha = \frac{b}{2\beta} \simeq \frac{\omega G(\omega) L(\omega) + \omega R(\omega) C}{2\omega\sqrt{L(\omega) C}} \tag{2.12}$$

$$\alpha \simeq \frac{G(\omega)}{2}\sqrt{\frac{L(\omega)}{C}} + \frac{R(\omega)}{2}\sqrt{\frac{C}{L(\omega)}} \tag{2.13}$$

This damping characteristic is shown in 11. Note that α is not linear with respect to frequency so the damping, like the dispersion, is variable with respect to frequency as well. For further details see [6].

2.3 SINGLE ENDED MEASUREMENT

The α and β define the damping and dispersion characteristics of a line propagation, $e^{(\alpha+j\beta)x}$ for a distance x from x_0. For a single ended measurement, the transmitter and receiver are

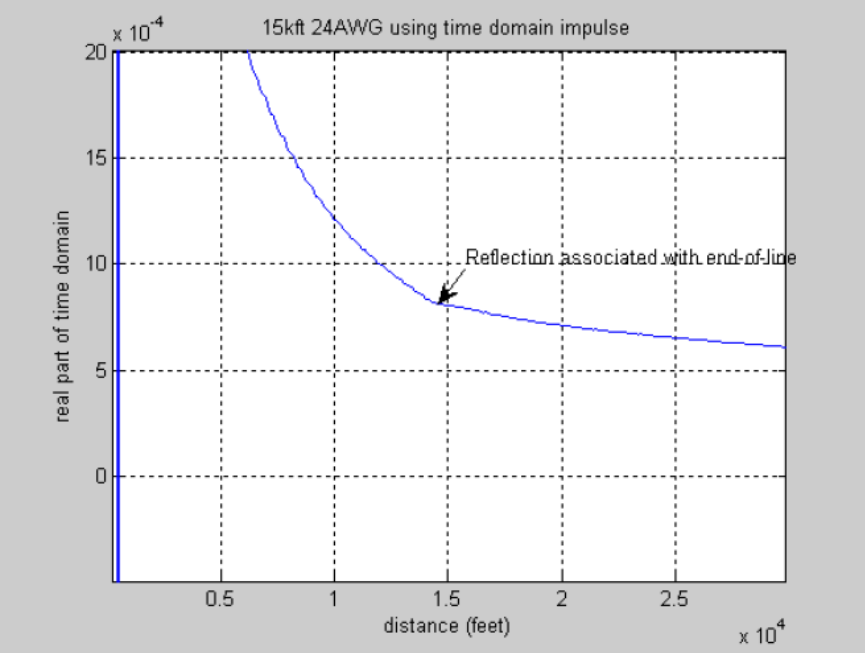

Figure 9: Zoomed in impulse in time of 15kft line in Figure 8

located at the same position x_0. The test equipment is usually set to a fixed source impedance and a fixed termination impedance. Most often the source and termination impedance are the same fixed value. This testing setup is shown in Figure 12.

In Figure 12, Z_T and Z_S are the receiver and source impedance respectively. The source impedance is the impedance that is visible at the output of the test equipment while transmitting. Likewise, the receiver impedance (or termination) is the impedance visible at the output of the test equipment while receiving. Since in a single ended measurement the test equipment is sending and receiving, both of these impedances are present on the line at the same time. Often times this is accomplished via a hybrid which allows transmit and receive to be done at the same time and with the same impedance presented to the line. The impedance is designed to be as close to the characteristic impedance of the line for the frequencies of interest. This is because matching the impedance allows for maximum power transfer to and from the line as well as allowing the least reflections, ρ_S and ρ_T . To further evaluate these reflections, we can look at the definition of a reflection coefficient with respect

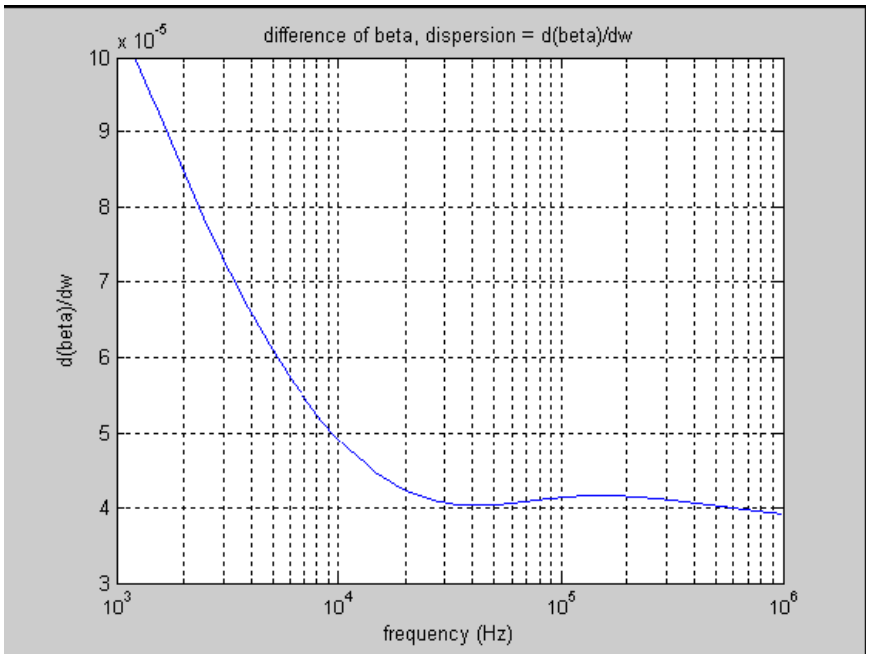

Figure 10: Dispersion over frequency

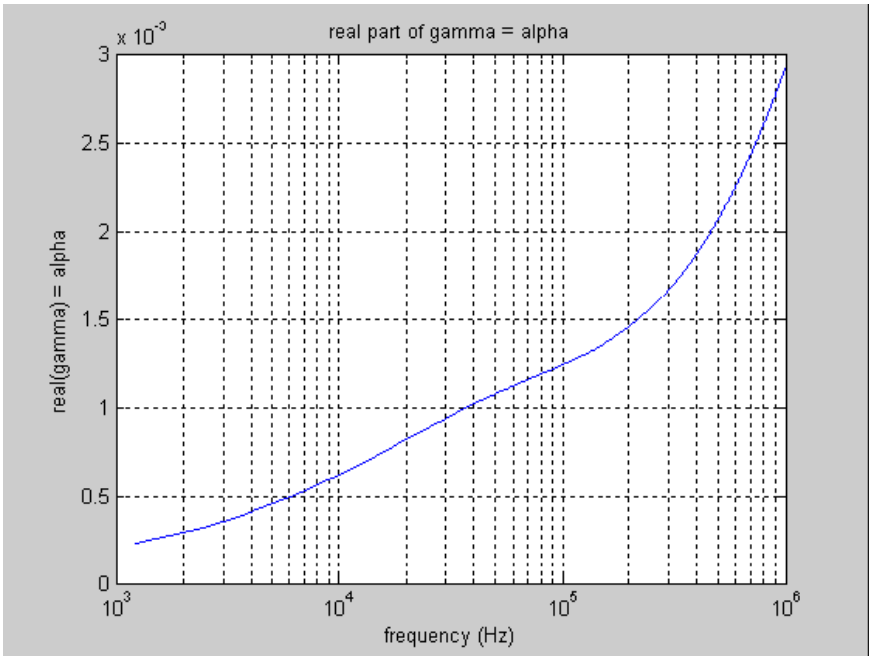

Figure 11: Alpha, real part of gamma

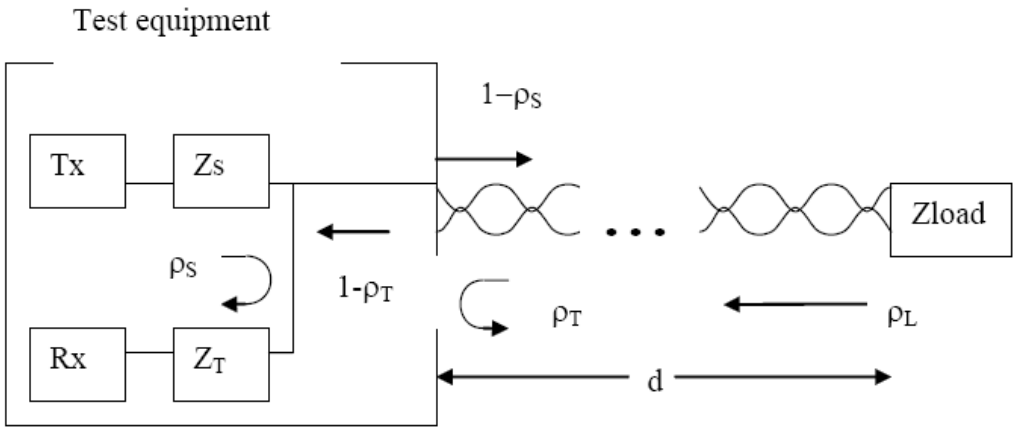

Figure 12: Single ended measurement setup

to the source. Sometimes called the S_{11} parameter, the reflection coefficient is defined as [1],

$$\rho_{meas} = \frac{Zin\,(\omega) - Zs}{Zin\,(\omega) + Zs}, \tag{2.14}$$

where $Zin(\omega)$ is the input impedance of the twisted pair and Zs is the source impedance used to drive the line. For twisted pair cable, the input impedance can be approximated as [1]:

$$Zin(\omega) = \frac{tanh(\gamma(\omega)d)Zo(\omega) + Zl(\omega)}{1 + tanh(\gamma(\omega)d)\frac{Zl(\omega)}{Zo(\omega)}}, \tag{2.15}$$

where $Zo(\omega) = \sqrt{\frac{R(\omega)+j\omega L(\omega)}{G(\omega)+j\omega C}}$ is the characteristic impedance of the twisted pair, $Zl(\omega)$ is the impedance of the load at the end of a twisted pair which can be a function of frequency, $\gamma(\omega) = \alpha(\omega)+j\beta(\omega)$ is the propagation characteristics of the twisted pair, and d is the length of the twisted pair shown in Figure 12. If we assume an open termination at Zload, then $Zl(\omega)$ becomes very large and $Zin(\omega)$ can be simplified to $Zin(\omega) = \frac{Zo(\omega)}{tanh(\gamma(\omega)d)}$. Plugging this back into equation 2.14 we have a reflection coefficient with an open at distance d of:

$$\begin{aligned}\rho_{open}(\omega) &= \frac{\frac{Zo(\omega)}{\tanh(\gamma(\omega)d)} - Zs}{\frac{Zo(\omega)}{\tanh(\gamma(\omega)d)} + Zs} = \frac{\frac{e^{2\gamma(\omega)d}+1}{e^{2\gamma(\omega)d}-1} \cdot \frac{Zo(\omega)}{Zs} - 1}{\frac{e^{2\gamma(\omega)d}+1}{e^{2\gamma(\omega)d}-1} \cdot \frac{Zo(\omega)}{Zs} + 1} \\ &= \frac{e^{2\gamma(\omega)d}\left(\frac{Zo(\omega)-Zs}{Zo(\omega)+Zs}\right) + 1}{e^{2\gamma(\omega)d} + \left(\frac{Zo(\omega)-Zs}{Zo(\omega)+Zs}\right)}\end{aligned} \tag{2.16}$$

but $\frac{Zo(\omega)-Zs}{Zo(\omega)+Zs}$ is the definition of the source reflection coefficient, $\rho_S(\omega)$, which is the energy that is reflected back into the test equipment at the output. Multiplying both numerator and denominator by $e^{-2\gamma(\omega)d}$ to get a damping relationship, equation 2.16 can also be written as:

$$\rho_{open}(\omega) = \frac{\rho_S(\omega) + e^{-2\gamma(\omega)d}}{1 + \rho_S(\omega)\, e^{-2\gamma(\omega)d}} \tag{2.17}$$

Similarly to the open termination, if we assume a short termination then $Zl(\omega)$ becomes very small and $Zin(\omega)$ can be simplified to $Zin(\omega) = tanh(\gamma(\omega)d)Zo(\omega)$. Plugging a short into equation 2.14 we have

$$\begin{aligned}\rho_{short}(\omega) &= \frac{tanh(\gamma(\omega)d)Zo(\omega) - Zs}{tanh(\gamma(\omega)d)Zo(\omega) + Zs} = \frac{\frac{e^{2\gamma(\omega)d}-1}{e^{2\gamma(\omega)d}+1} \cdot \frac{Zo(\omega)}{Zs} + 1}{\frac{e^{2\gamma(\omega)d}-1}{e^{2\gamma(\omega)d}+1} \cdot \frac{Zo(\omega)}{Zs} - 1} \\ &= \frac{e^{2\gamma(\omega)d}\left(\frac{Zo(\omega)-Zs}{Zo(\omega)+Zs}\right) - 1}{e^{2\gamma(\omega)d} - \left(\frac{Zo(\omega)-Zs}{Zo(\omega)+Zs}\right)}\end{aligned} \tag{2.18}$$

Similarly to equation 2.17, equation 2.18 can be rewritten as:

$$\rho_{short}(\omega) = \frac{\rho_S(\omega) - e^{-2\gamma(\omega)d}}{1 - \rho_S(\omega)\, e^{-2\gamma(\omega)d}} \tag{2.19}$$

Using a Zs of 120 ohms we can calculate the theoretical reflection coefficient. The magnitude and phase of the theoretical reflection coefficient are plotted in Figures 13 and 14. Then we can take the inverse Fourier transform of the reflection coefficients and view the real part giving an approximate impulse response of the loop. The result is plotted in Figure 15.

Suppose the source impedance (Zs) is matched to the characteristic impedance of the line (Zo), then the reflection coefficient becomes simple $Rc_{open}(\omega) = e^{-2\gamma(\omega)d}$ and $Rc_{short}(\omega) =$

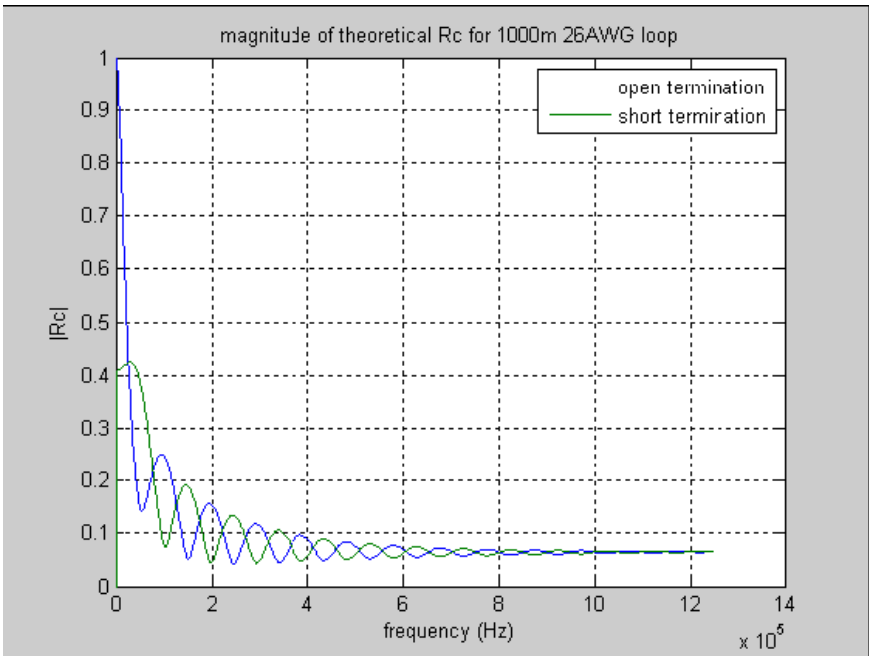

Figure 13: Theoretical magnitude of 1km 26AWG cable with open and short terminations

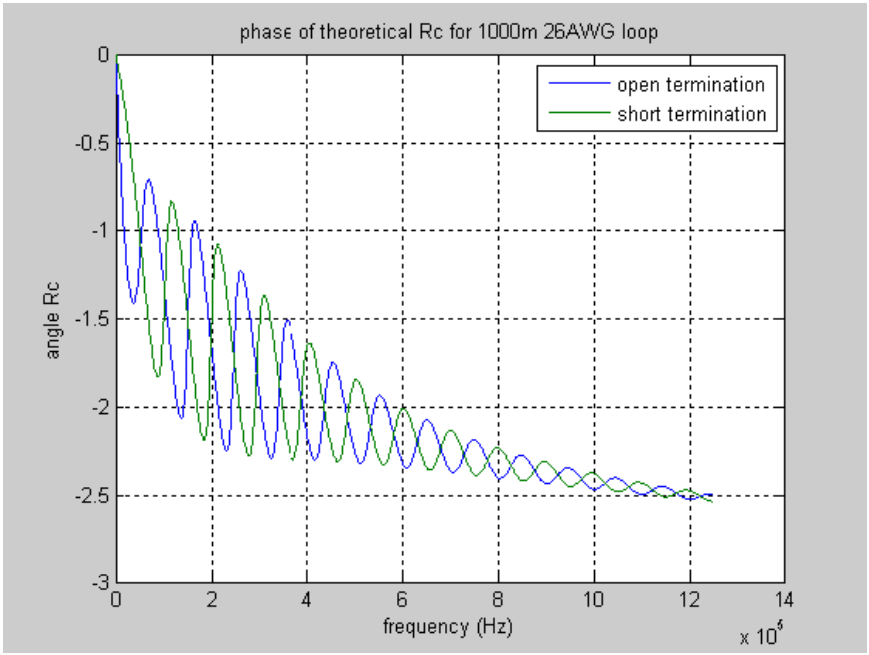

Figure 14: Theoretical phase of 1km 26AWG with open and short terminations

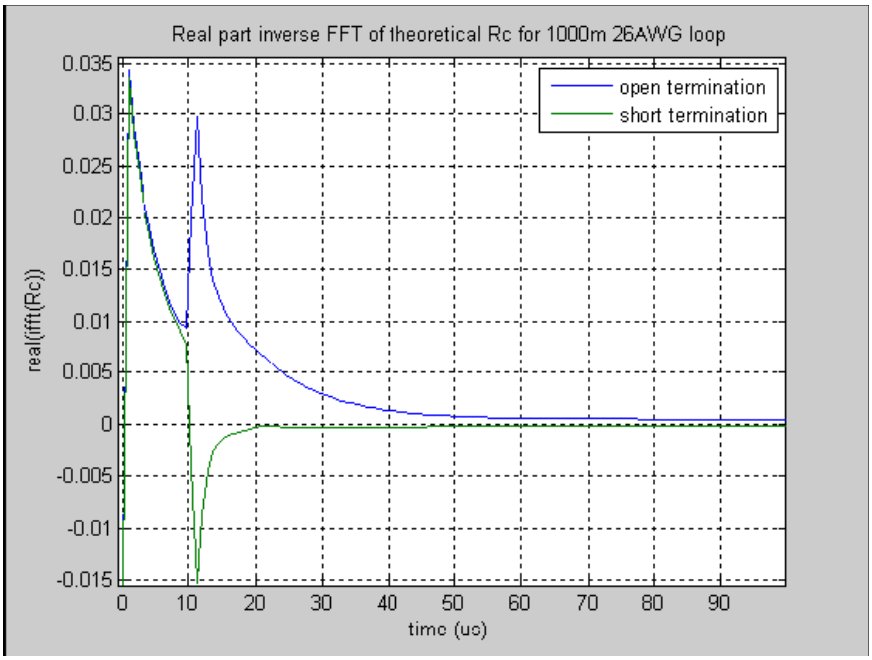

Figure 15: Real part IFFT of 1km 26AWG theoretical reflection coeff, open/short term

$-e^{-2\gamma(\omega)d}$. Notice the magnitudes are the same for an open and short in Figure 16, only the phase is different as is seen in Figure 17. The derivative of the phase is the same for the open and short termination cases. If we take an inverse Fourier transform of the reflection coefficient we can see the time relationship to distance of the open and the short, which is plotted in Figure 18.

Notice the exponential decay in Figure 15 is related to how well the source impedance is matched to the line impedance. In practice, matching the source impedance to the line is difficult and costly, so a nominal fixed impedance is generally chosen. For the frequencies ranging up to 1MHz, 100 ohms is often used. The positive going bump is related to the reflection caused by the open at the end of the line, and the negative going bump is related to the reflection caused by the short at the end of the line. In both matched and unmatched cases the open and short time domain plots are identical until a time that is related to the length of the line occurs. After which the open and short curves differ, whereby the open creates a positive going bump and the short creates a negative going bump.

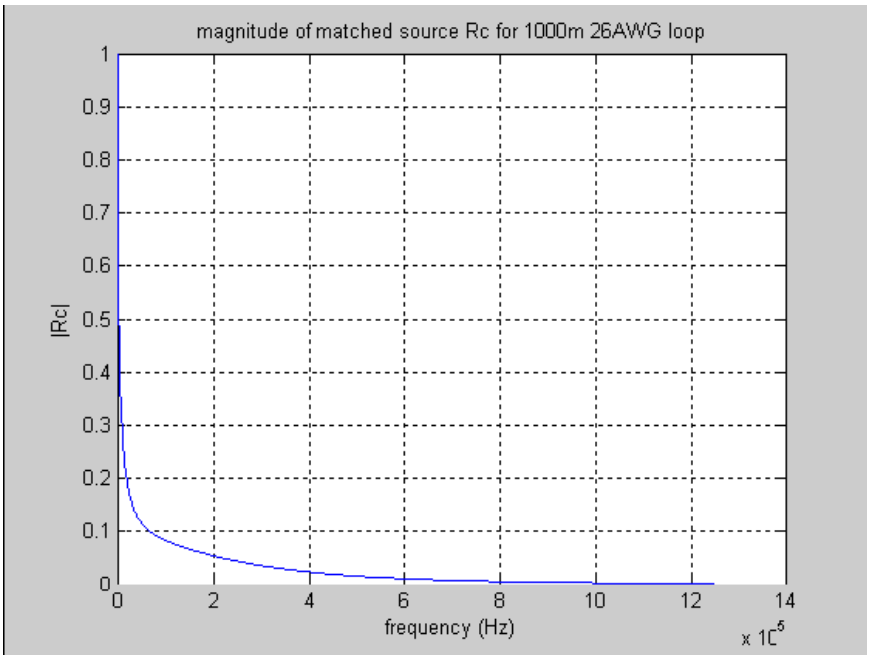

Figure 16: Matched source magnitude of 1km 26AWG cable, open/short term

2.4 INTUITIVE APPROACH TO SINGLE ENDED MEASUREMENT

If we look at how signals propagate using the test setup in Figure 12, we can follow the signal and add all the pieces of the signal that return to the receiver. the first of these pieces is the initial pulse multiplied by the source reflection, ρ_S. This is the signal that is immediately reflected into the receiver based on the source impedance isn't matched perfectly to the characteristic impedance of the line. For simplicity assume the initial pulse is 1 across all frequencies. Then the remainder of the signal, $(1-\rho_S(\omega))$, is sent to propagate through the loop with propagation characteristics $e^{-\gamma(\omega)x}$. Then if we assume there is an open termination at a distance d, the signal has full reflection at the open and the signal propagation becomes $e^{-2\gamma(\omega)d}$. The propagated signal is then split where a portion of the energy is absorbed into the receiver and another is reflected back into the loop to be propagated again. The portion that is absorbed by the receiver is $(1-\rho_S(\omega))e^{-2\gamma(\omega)d}(1-\rho_T(\omega))$. Adding this to the source

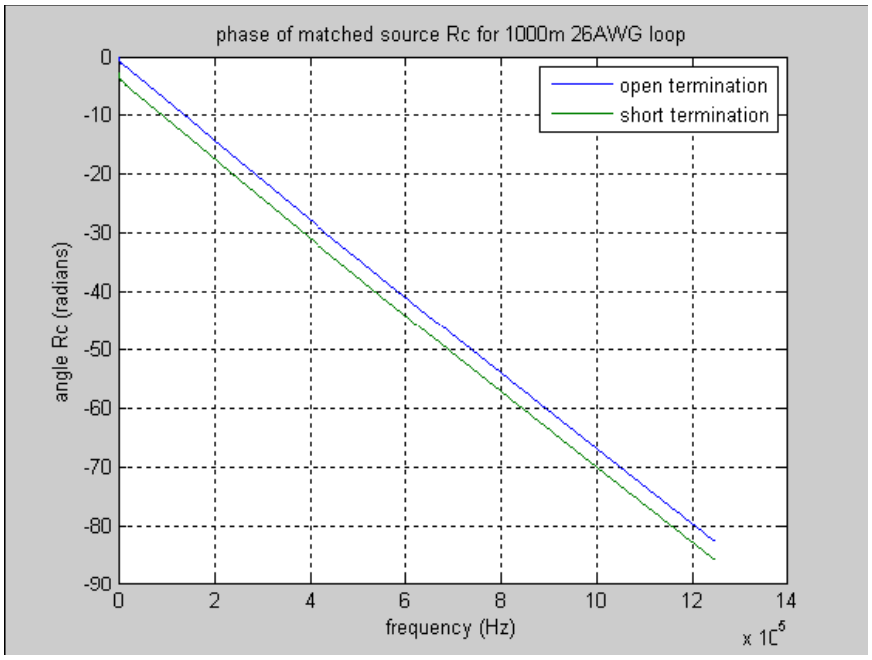

Figure 17: Matched source phase of 1km 26AWG cable, open/short term

reflection we have,

$$\rho_{open}(\omega) = \rho_S(\omega) + (1 - \rho_S(\omega))e^{-2\gamma(\omega)d}(1 - \rho_T(\omega)). \tag{2.20}$$

But the portion of the propagated signal is then propagated again and reflected at the open which then adds another term to the receiver.

$$\rho_{open}(\omega) = \rho_S(\omega) + (1 - \rho_S(\omega))e^{-2\gamma(\omega)d}(1 - \rho_T(\omega)) + (1 - \rho_S(\omega))e^{-4\gamma(\omega)d}\rho_T(\omega)(1 - \rho_T(\omega)). \tag{2.21}$$

This twice propagated signal again has some energy that is reflected back into the line and extrapolating to infinite reflections:

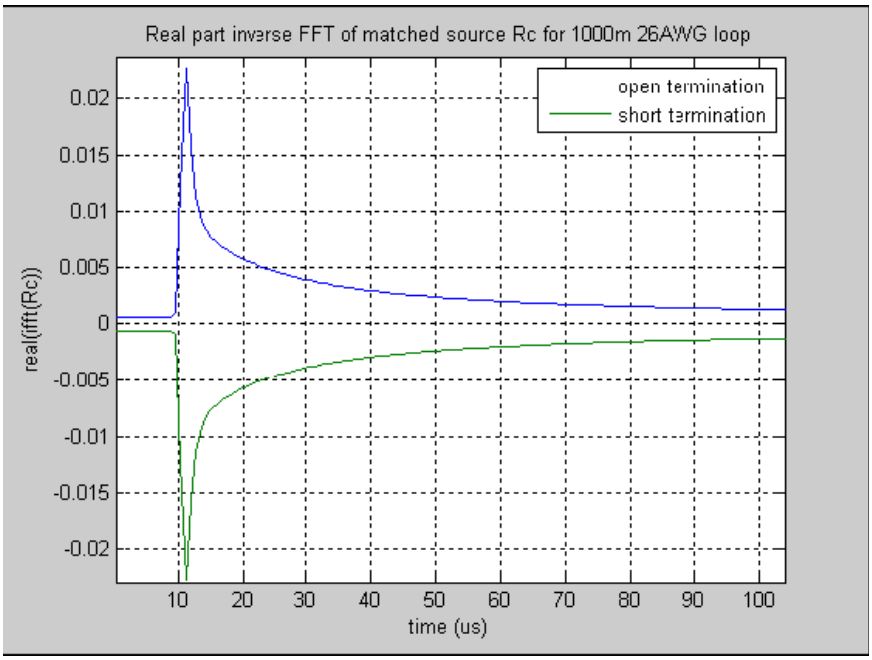

Figure 18: Matched source real part IFFT of 1km 26AWG cable, open/short term

$$\begin{aligned}
\rho_{open}(\omega) &= \rho_S(\omega) + (1-\rho_S(\omega))(1-\rho_T(\omega))e^{-2\gamma(\omega)d} + (1-\rho_S(\omega))(1-\rho_T(\omega))\rho_T(\omega)\, e^{-4\gamma(\omega)d} \\
&\quad +(1-\rho_S(\omega))(1-\rho_T(\omega))e^{-2\gamma(\omega)d}\left(\rho_T(\omega)\, e^{-2\gamma(\omega)d}\right)^2 \\
&\quad +(1-\rho_S(\omega))(1-\rho_T(\omega))e^{-2\gamma(\omega)d}\left(\rho_T(\omega)\, e^{-2\gamma(\omega)d}\right)^3 \\
&\quad +... \\
&= \rho_S(\omega) + (1-\rho_S(\omega))(1-\rho_T(\omega))e^{-2\gamma(\omega)d}\sum_{n=0}^{\infty}\left(\rho_T(\omega)\, e^{-2\gamma(\omega)d}\right)^n \qquad (2.22)
\end{aligned}$$

Twisted cable always has a damping effect whereby the real part of $e^{-2\gamma(\omega)d}$ is always less than 1. And by definition ρ_S is less than 1, so equation 2.22 can be simplified to

$$\rho_{open}(\omega) = \rho_S(\omega) + (1-\rho_S(\omega))(1-\rho_T(\omega))e^{-2\gamma(\omega)d}\frac{1}{1-\rho_T(\omega)e^{-2\gamma(\omega)d}}. \qquad (2.23)$$

Often times the test equipment is designed to transit and receive with the same impedance. If this is the case, ρ_S is equal to $-\rho_T$ and equation 2.23 can be further simplified to

$$\begin{aligned}\rho_{open}(\omega) &= \rho_S(\omega) + \frac{\left(1-\rho_S^2\left(\omega\right)\right)e^{-2\gamma(\omega)d}}{1+\rho_S\left(\omega\right)e^{-2\gamma(\omega)d}} \\ &= \frac{\rho_S\left(\omega\right)+e^{-2\gamma(\omega)d}}{1+\rho_S\left(\omega\right)e^{-2\gamma(\omega)d}}\end{aligned} \tag{2.24}$$

which is exactly equation 2.17.

Similarly for a short, an intuitive approach can be done. Except we need to consider what happens at the short at the end of length d. For a short, $\rho_L = -1$. So the propagation term will be negative, $-e^{-2\gamma(\omega)d}$, giving an infinite sum of

$$\begin{aligned}\rho_{short}(\omega) &= \rho_S(\omega) - (1-\rho_S(\omega))(1-\rho_T(\omega))e^{-2\gamma(\omega)d}\sum_{n=0}^{\infty}(-1)^n\left(\rho_T\left(\omega\right)e^{-2\gamma(\omega)d}\right)^n \\ &= \frac{\rho_S\left(\omega\right)-e^{-2\gamma(\omega)d}}{1-\rho_S\left(\omega\right)e^{-2\gamma(\omega)d}}\end{aligned} \tag{2.25}$$

which again is exactly equation 2.19. If the load $Zl(\omega)$ at distance d is unknown, then ρ_L of Figure 12 is also unknown and

$$\begin{aligned}\rho_{general}(\omega) &= \rho_S(\omega) + (1-\rho_S(\omega))(1-\rho_T(\omega))\rho_L\left(\omega\right)e^{-2\gamma(\omega)d}\sum_{n=0}^{\infty}\left(\rho_L\left(\omega\right)\right)^n\left(\rho_T\left(\omega\right)e^{-2\gamma(\omega)d}\right)^n \\ &= \frac{\rho_S\left(\omega\right)+\left(1-\rho_S\left(\omega\right)-\rho_T\left(\omega\right)\right)\rho_L\left(\omega\right)e^{-2\gamma(\omega)d}}{1-\rho_S\left(\omega\right)\rho_L\left(\omega\right)e^{-2\gamma(\omega)d}}\end{aligned} \tag{2.26}$$

and if we assume the source and receive impedances, Z_S and Z_T of the test equipment in Figure 12 are the same, then ρ_S is equal to $-\rho_T$ and we have

$$\rho_{general}(\omega) = \frac{\rho_S\left(\omega\right)+\rho_L\left(\omega\right)e^{-2\gamma(\omega)d}}{1-\rho_S\left(\omega\right)\rho_L\left(\omega\right)e^{-2\gamma(\omega)d}} \tag{2.27}$$

3.0 ELIMINATING DAMPING AND DISPERSION

3.1 MATCHED SOURCE AND RECEIVER IMPEDANCE

With reference to Figure 12, a simplified version of equation 2.27 has source impedance, Zs, equal to the receiver impedance, Zt, equal to the characteristic impedance of the line, Zo, then the source reflection is:

$$\rho_S(\omega) = \frac{Zs - Zo(\omega)}{Zs + Zo(\omega)} = 0 \tag{3.1}$$

and then equation 2.27 becomes:

$$\rho_{general}(\omega)_{matched} = \rho_L(\omega)\, e^{-2\gamma(\omega)d} \tag{3.2}$$

Simplifying further to examine open loads, we have $Zload = \infty$, which gives $\rho_L(\omega) = \frac{Zload - Z_0(\omega)}{Zload + Z_0(\omega)} = 1$; by which we have

$$\rho_{general}(\omega)_{open\_matched} = e^{-2\gamma(\omega)d} \tag{3.3}$$

This simplified reflection coefficient will be noted as $\rho_{om}(\omega)$. Taking the natural log we have:

$$log(\rho_{om}(\omega)) = -2\gamma(\omega)d \tag{3.4}$$

where $\gamma(\omega) = \sqrt{(R(\omega) + j\omega L(\omega))(G(\omega) + j\omega C)}$, and d is the distance to the open shown in Figure 12. Note that capacitance, C, is constant, but resistance, inductance and conductance are frequency dependent. Squaring and separating into real and imaginary parts, we have

$$\Re\left[\log\left(\rho_{om}(\omega)\right)\right]^2 = 4d^2\left(R(\omega)G(\omega) - \omega^2 L(\omega)C\right) \tag{3.5}$$

$$\Im\left[\log\left(\rho_{om}\left(\omega\right)\right)\right]^2 = 4d^2(\omega L(\omega)G(\omega) + \omega R(\omega)C) \tag{3.6}$$

However for North American (NA) cable types and frequencies ranging from 1kHz to 1MHz, from Figure 3, equation 3.5 and 3.6 can be approximated to:

$$\Re[log(\rho_{om}(\omega))]^2 \simeq 4d^2\left(-\omega^2 L(\omega)C\right) \tag{3.7}$$

$$\Im[log(\rho_{om}(\omega))]^2 \simeq 4d^2(\omega R(\omega)C) \tag{3.8}$$

For more information on the twisted-pair primary parameters, R, L, G, C, over frequency, ω, see tables 3.2, 3.3, and 3.4 of [2], also a condensed version is in Tables 1 and 2 in the Appendix. Now we define:

$$F_{re}\left(\omega\right) = \frac{\Re[log(\rho_{om}(\omega))]^2}{-4\omega^2 C} = d^2 L\left(\omega\right) \tag{3.9}$$

$$F_{im}\left(\omega\right) = \frac{\Im[log(\rho_{om}(\omega))]^2}{4\omega C} = d^2 R\left(\omega\right) \tag{3.10}$$

Taking the derivative of the log of these terms given:

$$\frac{d}{d\omega}\log F_{re}\left(\omega\right) = \frac{L'\left(\omega\right)}{L\left(\omega\right)} \tag{3.11}$$

$$\frac{d}{d\omega}\log F_{im}\left(\omega\right) = \frac{R'\left(\omega\right)}{R\left(\omega\right)} \tag{3.12}$$

For cable types similar to NA cables, $L(\omega)$ and $R(\omega)$ can be modeled as polynomials of ω defined as [3]:

$$L\left(\omega\right) = \sum_{n=0}^{4} l_n \omega^n \tag{3.13}$$

$$R\left(\omega\right) = \sum_{n=0}^{4} r_n \omega^n \tag{3.14}$$

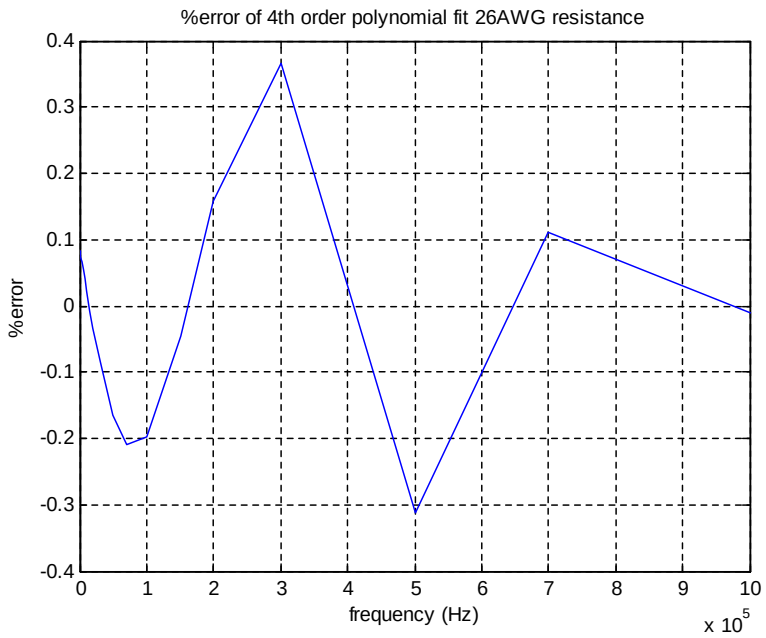

Figure 19: % error of resistance for 26 AWG twisted pair cable

Using the resistance and inductance values in Tables 3.3 and 3.4 in [2] and fitting to a 4th order polynomial we get a maximum resistance error of 0.37% and maximum inductance error of 0.29% for 26AWG PIC cable at 70 degrees F. Figures 19 and 20 show the % error over frequency.

Calculating $L'(\omega)$ and $R'(\omega)$, the coefficients with respect to l_0 and r_0 of the polynomials can be obtained. If we let $D_{re}(\omega) = \frac{d}{d\omega} \log F_{re}(\omega)$ and $D_{im}(\omega) = \frac{d}{d\omega} \log F_{im}(\omega)$, then

$$D_{re}(\omega) \sum_{n=0}^{4} l_n \omega^n = l_1 + 2l_2\omega + 3l_3\omega^2 + 4l_4\omega^3 \tag{3.15}$$

$$D_{im}(\omega) \sum_{n=0}^{4} r_n \omega^n = r_1 + 2r_2\omega + 3r_3\omega^2 + 4r_4\omega^3 \tag{3.16}$$

A minimum of 4 equations can be used to solve for $\frac{l_n}{l_0}$ and $\frac{r_n}{r_0}$ which can be substituted back into equations 3.9 and 3.10 and used to solve for distance d.

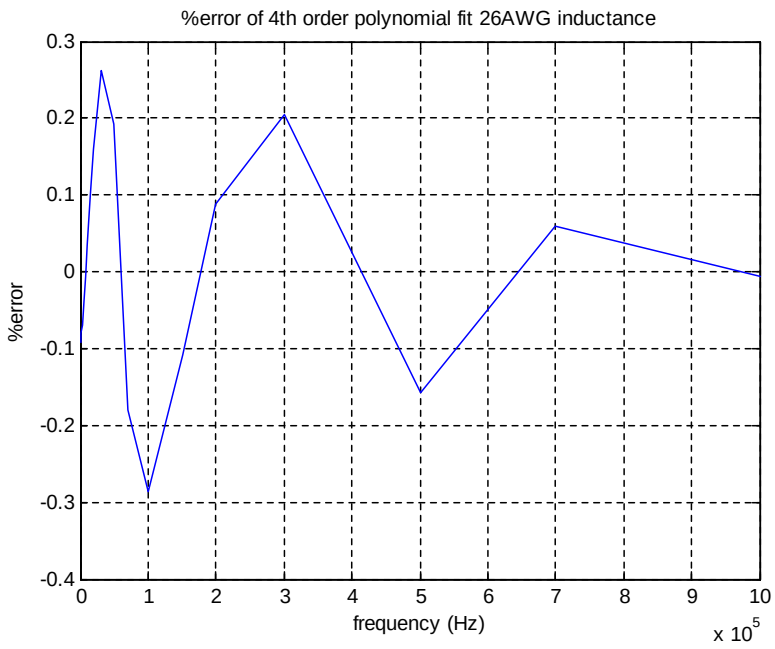

Figure 20: % error of inductance for 26AWG twisted pair cable

$$D_{re}(\omega) = (1 - D_{re}(\omega)\omega)\frac{l_1}{l_0} + \left(2\omega - D_{re}(\omega)\omega^2\right)\frac{l_2}{l_0} + \left(3\omega^2 - D_{re}(\omega)\omega^3\right)\frac{l_3}{l_0} \quad (3.17)$$
$$+ \left(4\omega^3 - D_{re}(\omega)\omega^4\right)\frac{l_4}{l_0}$$
$$D_{im}(\omega) = (1 - D_{im}(\omega)\omega)\frac{r_1}{r_0} + \left(2\omega - D_{im}(\omega)\omega^2\right)\frac{r_2}{r_0} + \left(3\omega^2 - D_{im}(\omega)\omega^3\right)\frac{r_3}{r_0} \quad (3.18)$$
$$+ \left(4\omega^3 - D_{im}(\omega)\omega^4\right)\frac{r_4}{r_0}$$

Looking at the inductance equation 3.17, $D_{re}(\omega)$ is measured and frequency, ω, is known for a given measurement. With frequencies measured as shown in Figure 3, we can solve $\frac{l_n}{l_0}$ in a least squares sense:

$$\begin{bmatrix} D_{re}(\omega_1) \\ D_{re}(\omega_2) \\ \dots \\ D_{re}(\omega_N) \end{bmatrix} = \begin{bmatrix} (1 - D_{re}(\omega_1)\omega_1) & (2\omega_1 - D_{re}(\omega_1)\omega_1^2) & \dots & (6\omega_1^3 - D_{re}(\omega_1)\omega_1^4) \\ (1 - D_{re}(\omega_2)\omega_2) & (2\omega_2 - D_{re}(\omega_2)\omega_1^2) & \dots & (6\omega_2^3 - D_{re}(\omega_2)\omega_2^4) \\ \dots & \dots & \dots & .. \\ (1 - D_{re}(\omega_N)\omega_N) & (2\omega_N - D_{re}(\omega_N)\omega_N^2) & \dots & (6\omega_N^3 - D_{re}(\omega_N)\omega_N^4) \end{bmatrix} \cdot \begin{bmatrix} \frac{l_1}{l_0} \\ \frac{l_2}{l_0} \\ \frac{l_3}{l_0} \\ \frac{l_4}{l_0} \end{bmatrix} \tag{3.19}$$

$$\mathbf{D}_{re} = \tilde{\mathbf{D}_{re}} \cdot \mathbf{L}/l_0 \tag{3.20}$$

Solving for $\mathbf{L}/l_0$,

$$\mathbf{L}/l_0 = \left(\tilde{\mathbf{D}_{re}^T}\tilde{\mathbf{D}_{re}}\right)^{-1} \tilde{\mathbf{D}_{re}^T}\mathbf{D}_{re} \tag{3.21}$$

and similarly for $\mathbf{R}/r_0$,

$$\mathbf{R}/r_0 = \left(\tilde{\mathbf{D}_{im}^T}\tilde{\mathbf{D}_{im}}\right)^{-1} \tilde{\mathbf{D}_{im}^T}\mathbf{D}_{im} \tag{3.22}$$

Now equations 3.9 and 3.10 can be re-written as

$$F_{re}(\omega) = d^2 l_0 \sum_{n=0}^{4} \frac{l_n}{l_0}\omega^n \tag{3.23}$$

$$F_{im}(\omega) = d^2 r_0 \sum_{n=0}^{4} \frac{r_n}{r_0}\omega^n \tag{3.24}$$

where $\frac{l_n}{l_0}$ and $\frac{r_n}{r_0}$ are known from solving equations 3.21 and 3.22. Distance, d, for typical North American twisted pair lines range from 300m to 6km, the base inductance, l_0, ranges from 617 - 675 x 10^{-9} $H/meter$, and the base resistance, r_0, ranges from 0.1746 - 0.2862 $\Omega/meter$. If we use an average l_0 of 646.3 x 10^{-9} $H/meter$, then we can solve for $L(\omega)$,

$$L(\omega) = l_0 \sum_{n=0}^{4} \frac{l_n}{l_0}\omega^n \tag{3.25}$$

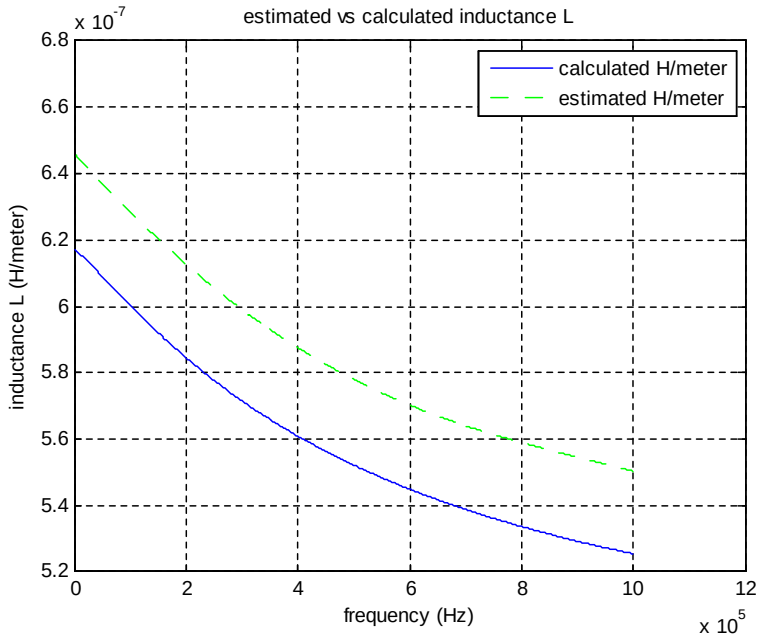

Figure 21: Estimated inductance from 4kft 24AWG line and calculated inductance

Using a simulated 4kft loop of 24AWG with matched source impedance, we get an estimated $L(\omega)$ shown in Figure 21.

Then substituting the estimated inductance $L(\omega)$ into equation 3.9, we can solve for an estimated distance d_{est}. This estimation for a 4kft 24AWG loop is shown in Figure 22 and has a mean value of 1191.6 meters or 3.909kft. This estimation is off by approximately 2.3% from the actual length of 4kft. Using the estimated distance to calculate the resistance $R(\omega) = \frac{F_{im}}{est\_d(\omega)^2}$, we get an estimated resistance shown in Figure 23. If we start by assuming a nominal resistance r_0 value of 0.2304, rather than a nominal inductance l_0 value, we get an estimated $R(\omega)$ shown in Figure 24.

The error from the estimated resistance from the calculated resistance is much greater in Figure 24 than in Figure 23. Furthermore, when substituting the estimated resistance $R(\omega)$ into equation 3.10, then solving for an estimated distance d, we get a mean value of 1061.9 meters or 3.483kft which is off by approximately 13% from the actual length of 4kft. Using this estimated distance from the estimated resistance, we can estimate the inductance using

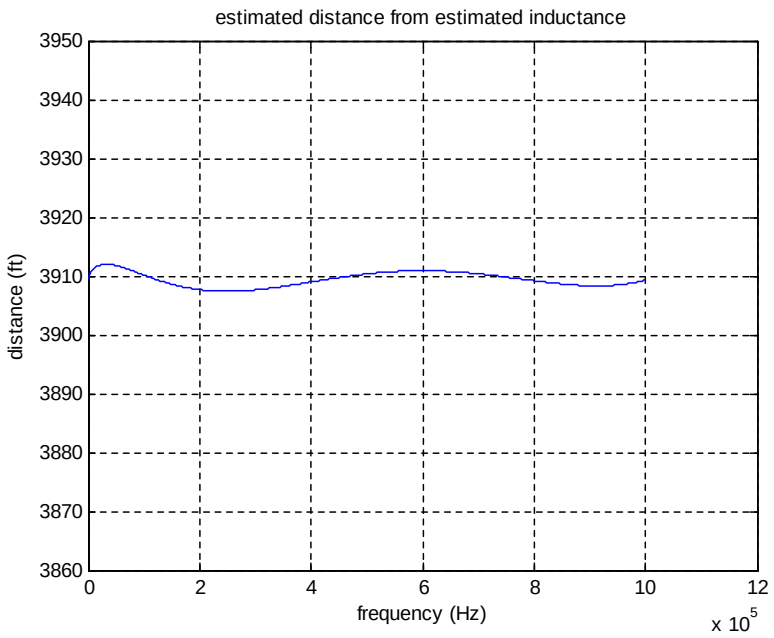

Figure 22: Estimated distance for 4kft 24AWG line using nominal inductance

the estimated distance to calculate the inductance $L(\omega) = \frac{F_{re}}{est\_d(\omega)^2}$, getting an estimated inductance shown in Figure 25.

The error in Figure 25 is much greater than the error in Figure 21. So in conclusion, the better method is to use the nominal value of the "DC" inductance, $l_0 = 646.3x10^{-9} H/meter$, and solve the estimated resistance, $R(\omega)$, from the estimated inductance. Similarly for 4kft of 26AWG we obtain an estimated resistance and inductance as seen in Figures 26 and 27.

Figure 26 shows a larger deviation at very low frequencies. So the estimation is better when a subset of the measured frequencies are used for the estimation. In general, estimation with 40kHz to 1MHz frequencies gives a more stable result. Then with the estimated resistance and inductance we can calculate the estimated propagation γ

$$\gamma_{est}(\omega) = \sqrt{-\omega^2 L_{est}(\omega) C + j\omega R_{est}(\omega) C} \quad (3.26)$$

$$= \alpha_{est}(\omega) + j\beta_{est}(\omega) \quad (3.27)$$

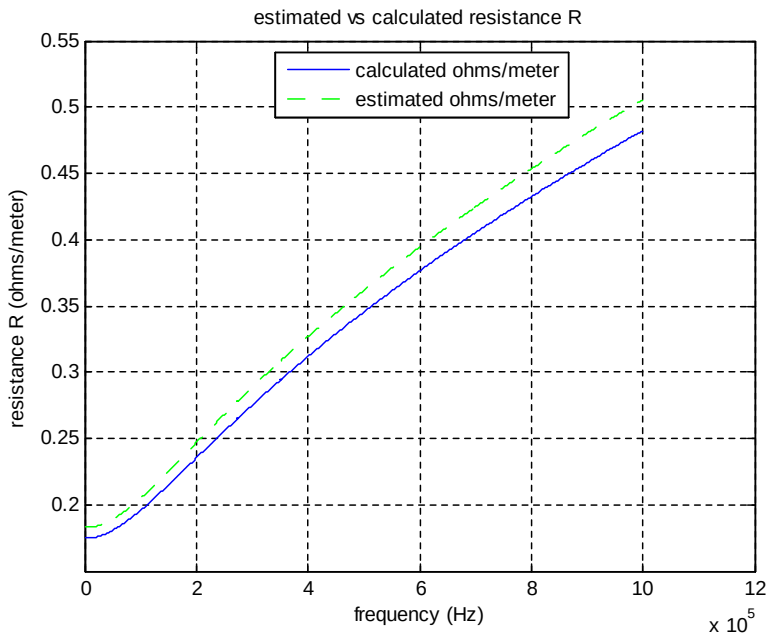

Figure 23: Estimated resistance using nominal inductance vs calculated resistance

based on the same approximations done on 3.5 and 3.6. Looking at the reflection coefficient with a matched source impedance, we can separate out the damping and dispersion parts of the propagation.

$$\rho_{general}(\omega)_{matched} = \rho_L(\omega)\, e^{-2(\alpha(\omega)+j\beta(\omega))d} \tag{3.28}$$

Then, assuming the measured reflection coefficient has matched impedance, we can divide the measured reflection coefficient by the damping portion, α, of the propagation,

$$\frac{\rho(\omega)_{mesured}}{e^{-\alpha(\omega)2d}} = \rho_L(\omega)\, e^{-j\beta(\omega)2d} \tag{3.29}$$

$$\rho_{scaled}(\omega) = \frac{\rho(\omega)_{mesured}}{e^{-\alpha_{est}(\omega)2d_{est}}} \tag{3.30}$$

leaving the location of the impedance mismatch including damping and the impedance mismatch reflection coefficient. Figure 28 shows the result $\rho_{scaled}(\omega)$ for various open impedance mismatch locations. The peaks and shape for each mismatch location are very similar with

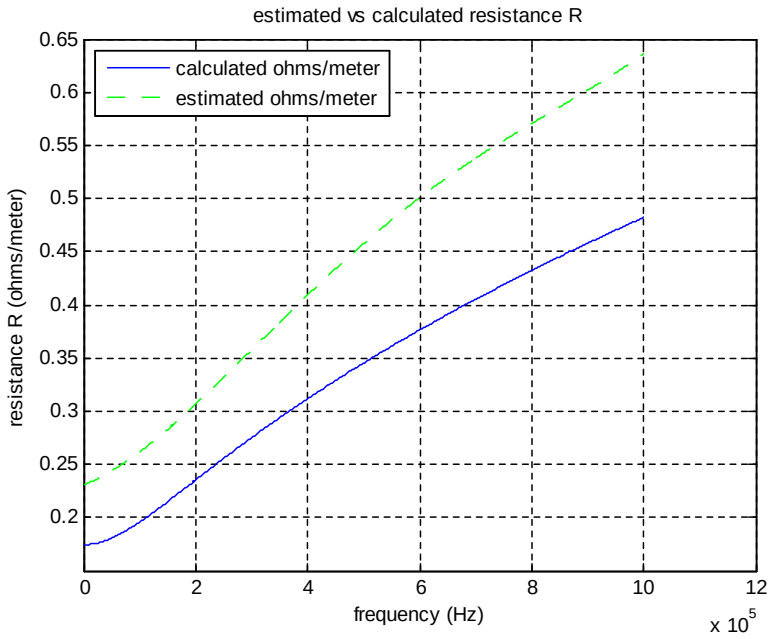

Figure 24: Estimated resistance using nominal resistance vs calculated resistance

a slight decrease in amplitude and slight spreading of the peak. This is in contrast to unprocessed reflection coefficients for the same impedance mismatch locations as is shown in Figure 29. The location of the peaks in Figure 28 show an approximately linear relationship between propagation time and impedance mismatch distance. Figure 30 plots the distance vs. time location of the peak, which gives an approximate propagation time of $0.321\mu\sec/kft$. While Figure 28 still has some dispersion, shown in the slight spreading of the peak, it does not appear to be enough to cause the propagation time for distances up to 15kft to be non-linear.

While dispersion is not problematic in this application, the spreading of the pulse could cause two closely located impedance discontinuities to merge into one pulse with two peaks or one peak centered between the locations. A possible remedy is to process further to account for the dispersion. $\beta(\omega)$ could be fit to a line where the imaginary part of the propagation is approximately linear. From Figure 10, frequencies 20kHz and above are approximately linear, so a line could be fit to the estimated $\beta(\omega)$ for $\omega \succeq 2\pi 20kHz$. Fitting the line to theoretical $\beta(\omega)$, we can compare the derivatives in Figure 31. Then the difference from the

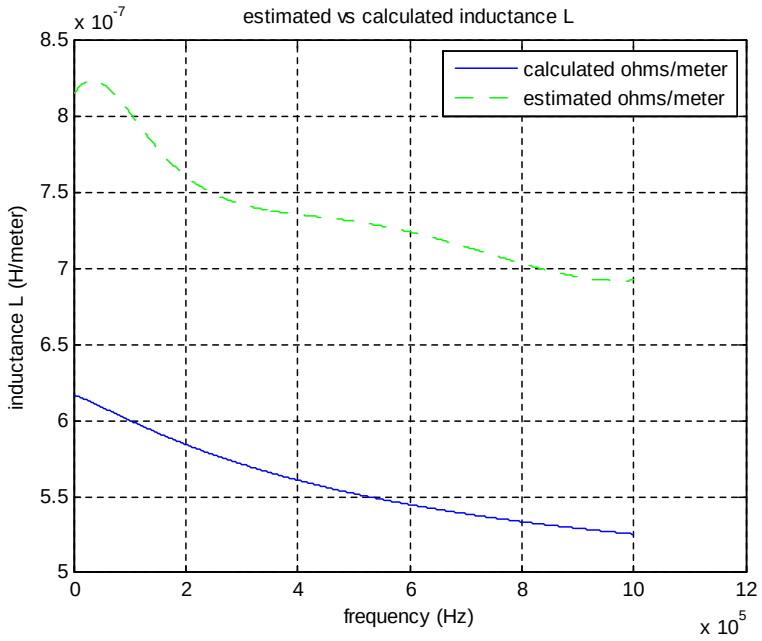

Figure 25: Estimated inductance using nominal resistance vs calculated inductance

line fit to the estimated $\beta(\omega)$ can be described as a function of frequency $g(\omega)$. The scaled reflection coefficients, 3.30, can be further scaled for dispersion by multiplying by $e^{j2dg(\omega)}$.

$$g(\omega) = \beta(\omega) - lineFit(\omega) \tag{3.31}$$

$$\frac{\rho(\omega)_{mesured}}{e^{-\alpha(\omega)2d}} e^{j2dg(\omega)} = \rho_L(\omega) e^{-j\beta(\omega)2d} e^{-j2dg(\omega)} \tag{3.32}$$

$$= \rho_L(\omega) e^{-j2d(lineFit(\omega))} \tag{3.33}$$

Applying this to measured data we get:

$$\rho_{scaled\_disp}(\omega) = \frac{\rho(\omega)_{mesured}}{e^{-\alpha_{est}(\omega)2d_{est}}} e^{jg(\omega)2d_{est}} \tag{3.34}$$

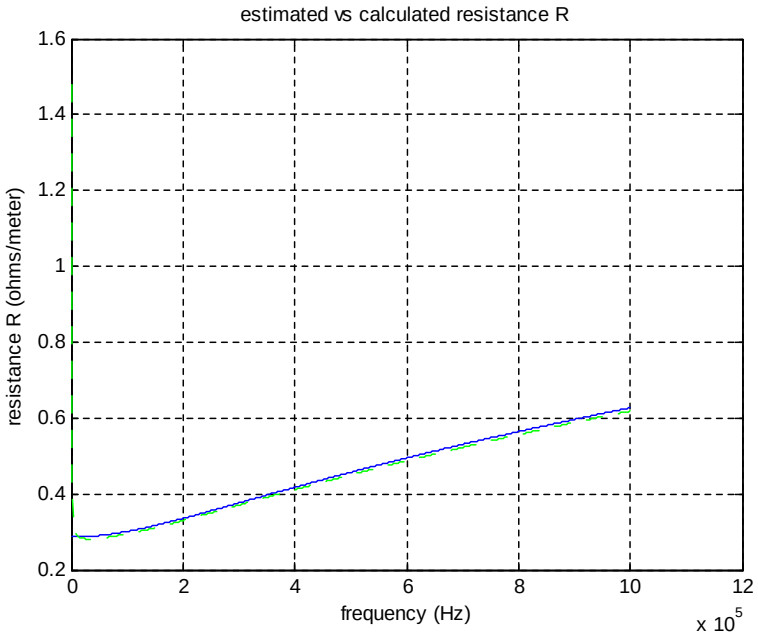

Figure 26: Estimated inductance using nominal inductance for 26AWG cable

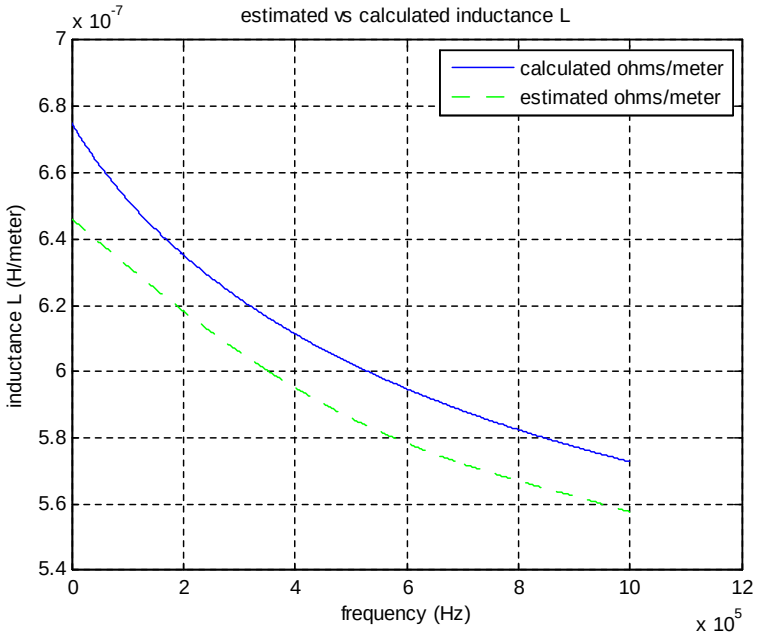

Figure 27: Estimated inductance using nominal inductance for 26AWG cable

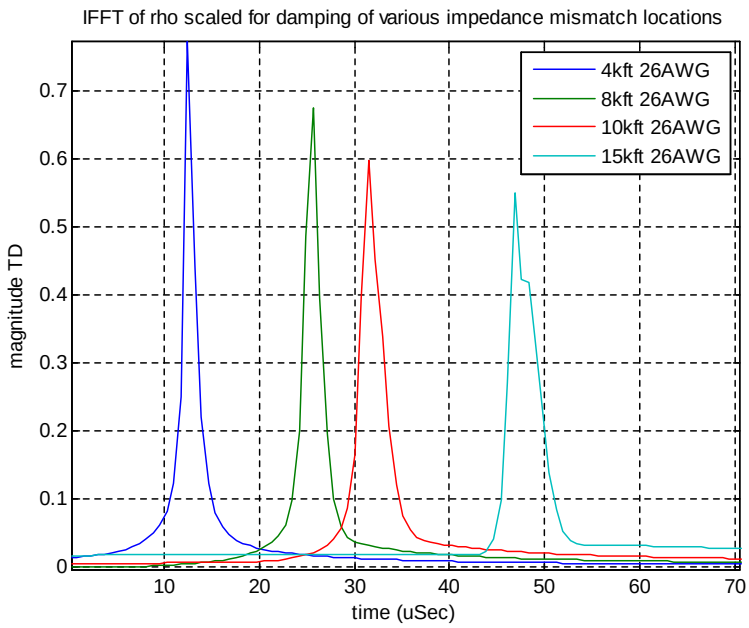

Figure 28: Impedance mismatch locations, damping scaled by estimated propagation

3.2 UNMATCHED SOURCE AND RECEIVER IMPEDANCE

In practical applications, creating a test equipment with matched source impedance to the cable characteristic impedance is difficult and often impractical. So we need to consider an unmatched source impedance. Feeding the fixed source impedance reflection coefficient into the estimation algorithm without pre-processing gives very poor matching. Figure 32 shows the results of the estimating resistance from reflection coefficients with 120 ohms source and terminating impedance.

Figure 32 clearly shows the unmatched source impedance reflection coefficient cannot be directly used for estimating the propagation. However, if we know what type of cable we need to match, we can calculate what the reflection coefficients would be with a matched input impedance by calculating ρ_S which is defined as

$$\rho_S(\omega) = \frac{Zs - Zo(\omega)}{Zs + Zo(\omega)} \tag{3.35}$$

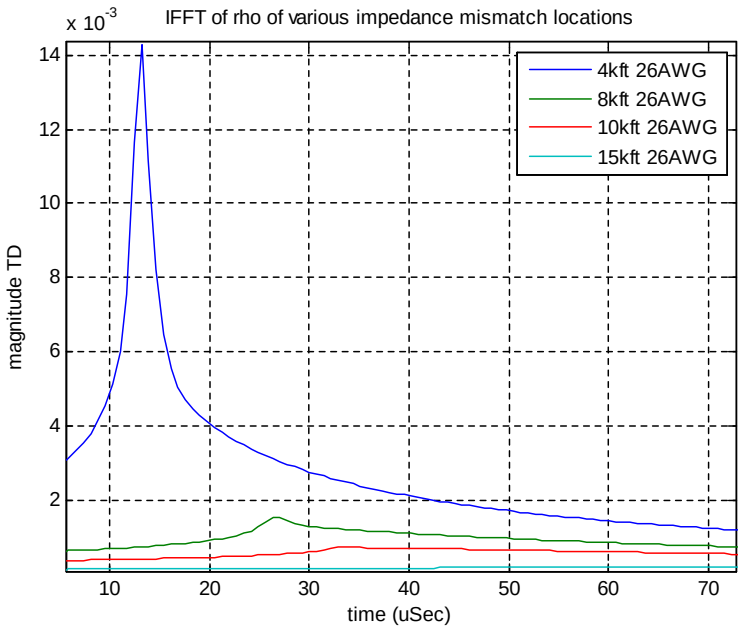

Figure 29: Impedance mismatch locations without damping normalization

If we assume the starting cable type is 26AWG, which often times in NA this is the case, then $Zo(\omega)$ can be calculated.

$$Zo\left(\omega\right)_{26} = \sqrt{\frac{R\left(\omega\right)_{26} + j\omega L\left(\omega\right)_{26}}{G\left(\omega\right)_{26} + j\omega C}} \tag{3.36}$$

Then if we create a test fixture with a known source impedance that matches the terminating impedance we can calculate the source reflection, $\rho_S\left(\omega\right)$. With the source reflection known, we can solve for the propagation effects and the load reflection, $\rho_L\left(\omega\right)e^{-2\gamma(\omega)d}$ from 2.27.

$$\rho_L\left(\omega\right)e^{-2\gamma(\omega)d} = \frac{\rho_{general}(\omega) - \rho_S\left(\omega\right)}{1 + \rho_S\left(\omega\right)\rho_{general}(\omega)} \tag{3.37}$$

$$\rho_{adj}\left(\omega\right) = \frac{\rho_{meas}(\omega) - \rho_S\left(\omega\right)}{1 + \rho_S\left(\omega\right)\rho_{meas}(\omega)} \tag{3.38}$$

The estimated resistance using the adjusted reflection coefficient $\rho_{adj}\left(\omega\right)$ is a much closer match to the calculated resistance as shown in Figure 33.

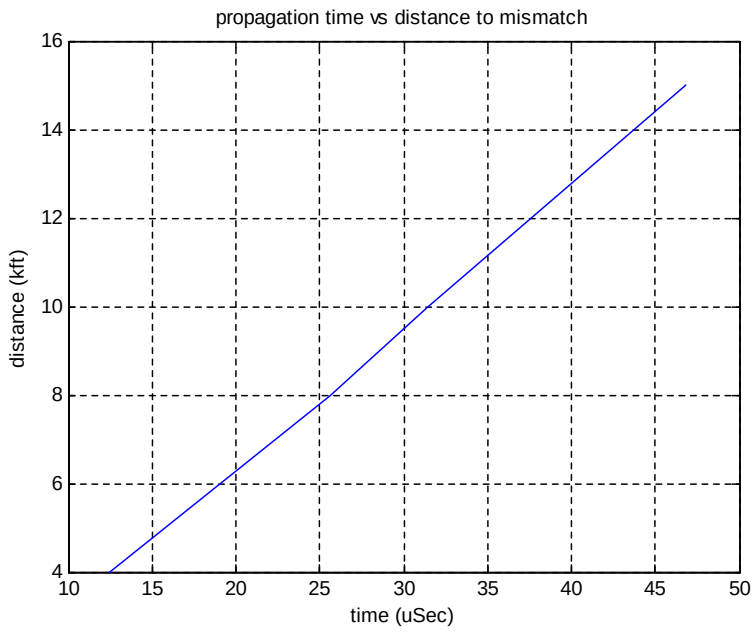

Figure 30: Time location of peaks vs impedance location distance

This adjusted reflection coefficient gives a processed and scaled reflection peak for the 4kft location at 12.43us, the same location as the scaled reflection peak with matched impedance shown in Figure 28. A plot of the adjusted reflection coefficient scaled for damping with the estimated propagation and estimated distance using equation 3.30 is shown in Figure 34 matching closely with Figure 28.

3.3 NOISE CONSIDERATIONS

Noise levels in twisted pair testing need to be very low. This is because losses for frequencies above voice frequencies (3.4kHz and above) are quite large. To get a true idea of what kind of noise levels are needed, we took a field collected reflection coefficient measurement and extracted only the noise from the signal in the time domain and took a Fourier transform to get the frequency levels of the noise. Figure 35 shows the results of that process leaving just the noise component of the signal.

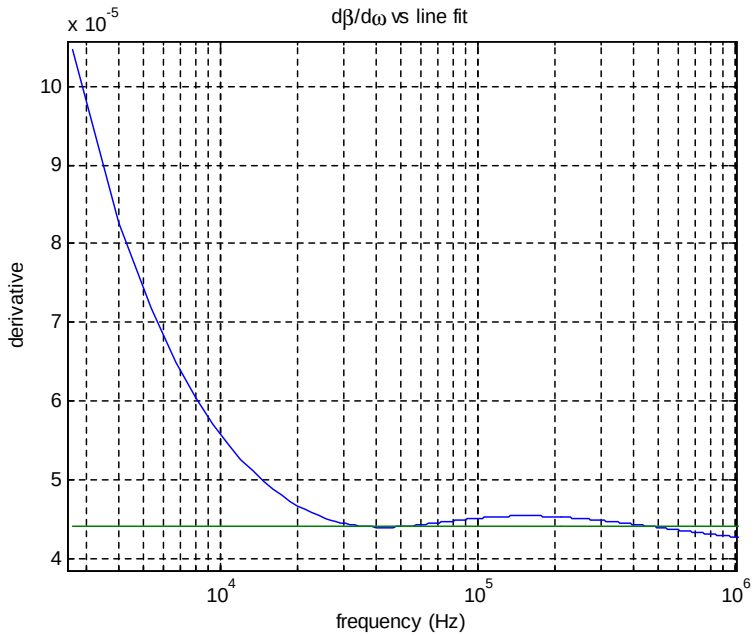

Figure 31: Derivative of beta with respect to omega vs line fit

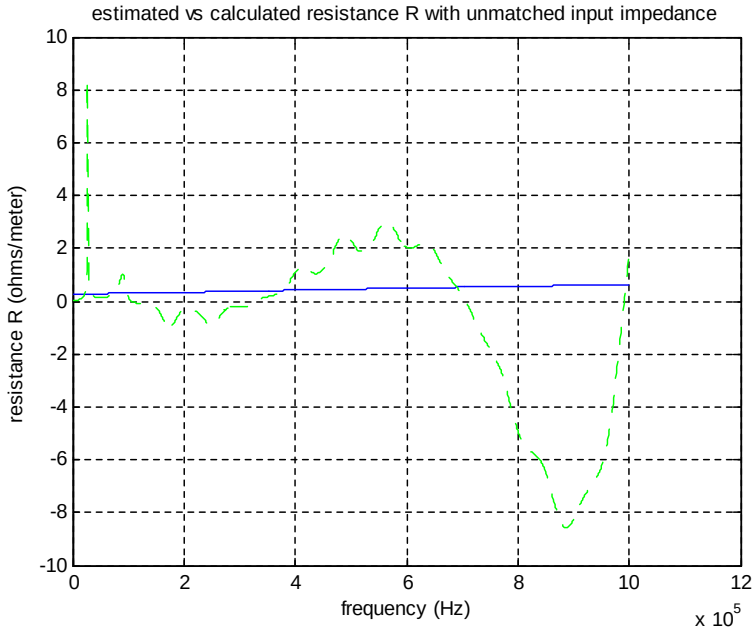

Figure 32: Estimated resistance of reflection coefficient with 120 ohms source

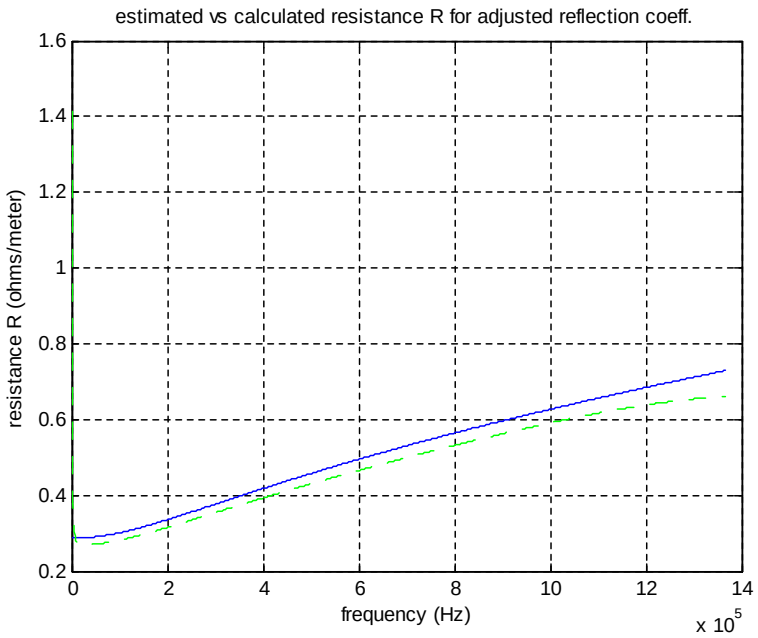

Figure 33: Estimated resistance of reflection coefficient adjusted for 120 ohms source

The pre-processing involves tight differential measurements along with long sampling times to gain the magnitude and phase shift of the received signal with respect to the transmitted signal. An example of pre-processing of the reflection coefficient is illustrated in [3]. Notice also this noise is not flat, but follows the loss associated with the twisted pair cable. So to define the proposed method's sensitivity to noise we must consider a non-white noise as well. To do this, we can create white noise in the frequencies of interest and attenuate the noise to follow a similar trend as the field collected noise. In Figure 36, noise is added that follows the profile in Figure 35 and has a SNR of 27dB for 4kft, 17dB for 8kft, and 14dB for 10kft. The 15kft loop did not estimate correctly for added noise. SNR was calculated as follows:

$$SNR_{dB} = 10\log_{10}\frac{\sum_f \left|\rho_{sig}\left(\omega_f\right)\right|^2}{\sum_f \left|noise\left(\omega_f\right)\right|^2} \tag{3.39}$$

But if we assume we have an unmatched source for $\rho_{sig}\left(\omega_f\right)$, which is often the case in practice, then the SNR for the noise shown in 36 is approximately 30dB for all distances.

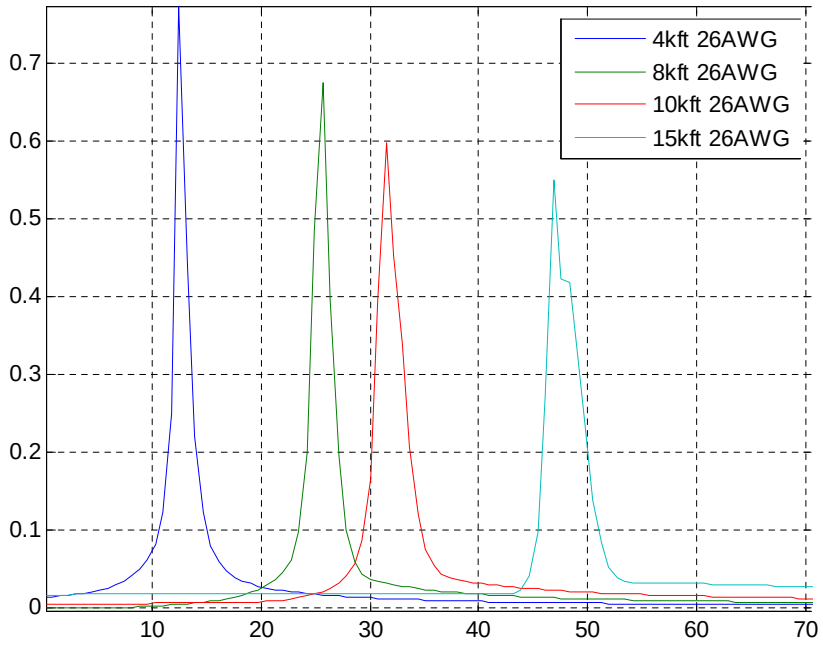

Figure 34: Impedance mismatch locations, source reflection adjusted, damping normalized

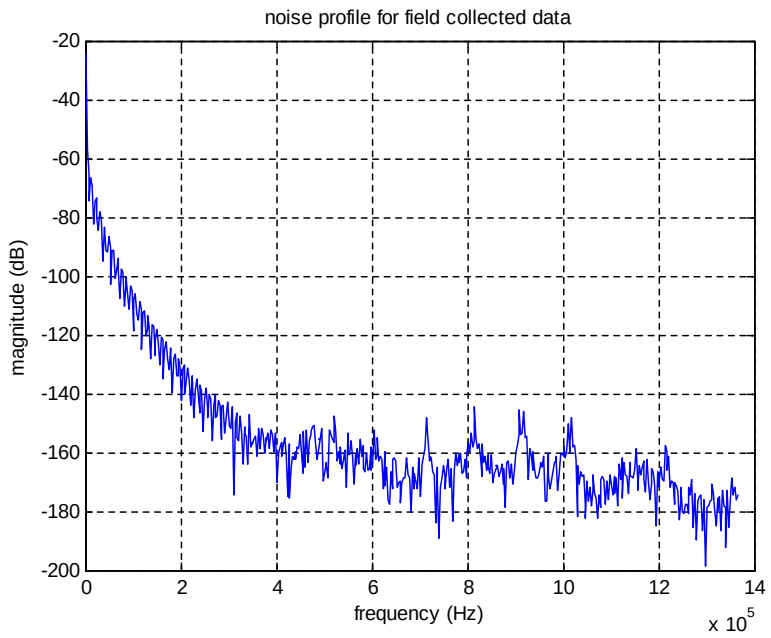

Figure 35: Residual noise, field collected reflection coefficient

This change is because when there is an unmatched source the energy level of the source reflection is greater than the propagation.

If we instead add flat white noise to an unmatched source, we need to have a much greater SNR to maintain functionality. This is because the upper frequencies are attenuated significantly from the lower frequencies so that for those upper frequencies the SNR is greatly reduced and can even have noise exceeding the level of the signal if the noise is flat. For instance, the frequency 300kHz, which is a commonly used as a gauge to determine the health of a ADSL line, has losses of ~4.41dB per kft for 26AWG. For a 15kft 26AWG line, the loss is >60dB, for equipment located only at one end this loss exceeds 120dB. Figure 37, shows a comparison of a 4kft 26AWG line with no noise and with 60dB SNR white noise added. To

understand why the algorithm fails for increased white noise we can look at the estimated propagation. Figure 38 shows a comparison of the real part of the estimated gamma, α, for 4kft 26AWG with no noise and with 60dB SNR flat noise added. There is quite a deviation from the non-noise estimated gamma, but from Figure 37 the algorithm still indicates the

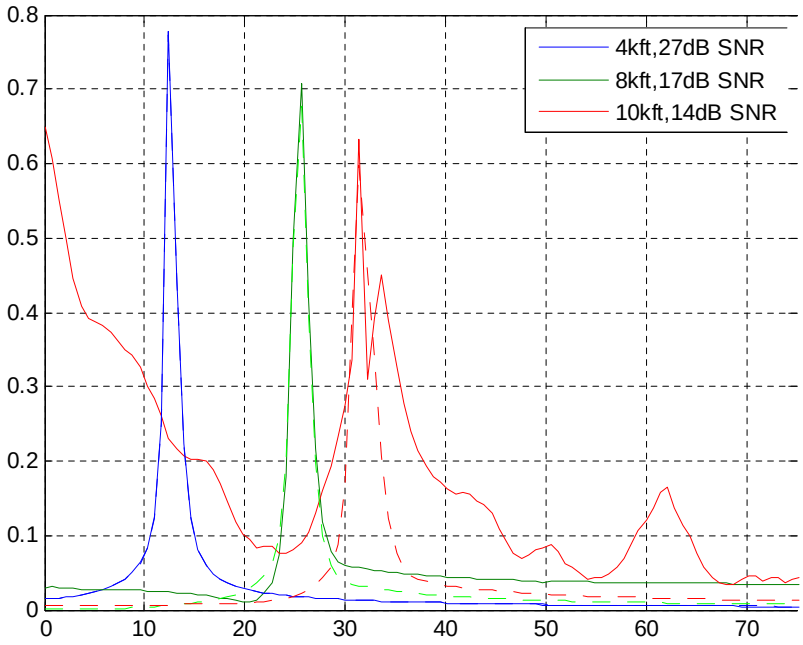

Figure 36: Field noise added to source matched rho scaled for damping

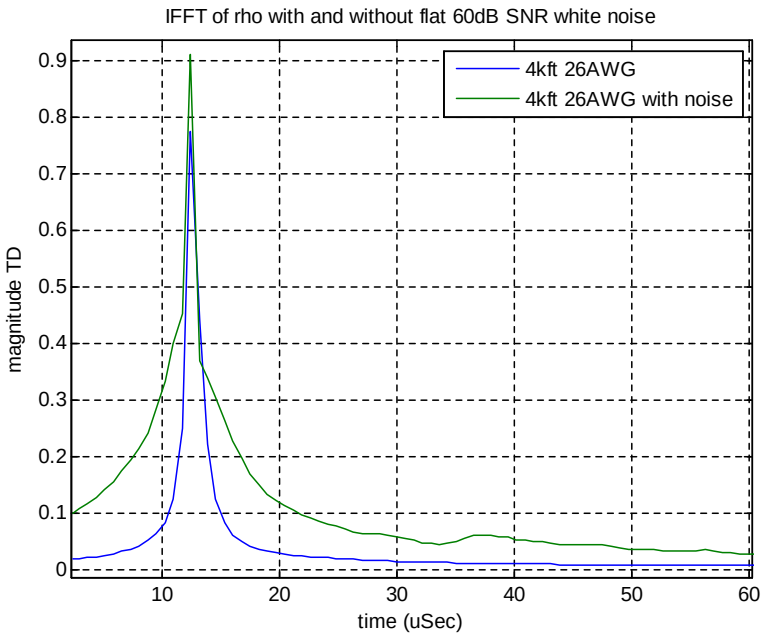

Figure 37: IFFT of scaled reflection coefficient with added white noise

correct location of the impedance discontinuity.

If we lower the SNR of the flat white noise source further to 50dB, the algorithm falls apart. Figure 39 shows the deviation of the real part of the estimated gamma to be quite severe. As expected, with added white noise, the upper frequencies suffer the most because the propagated signal is lower as the frequency increases. In this case with 50dB of white noise added, the estimation propagation error from the actual propagation is too great to scale the reflection coefficients for damping.

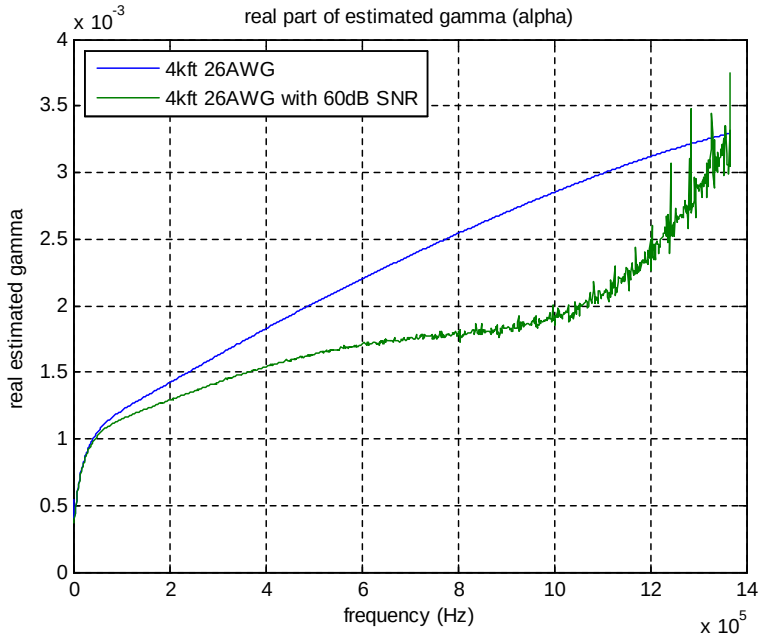

Figure 38: Real part of estimated propagation, 60dB SNR flat white noise

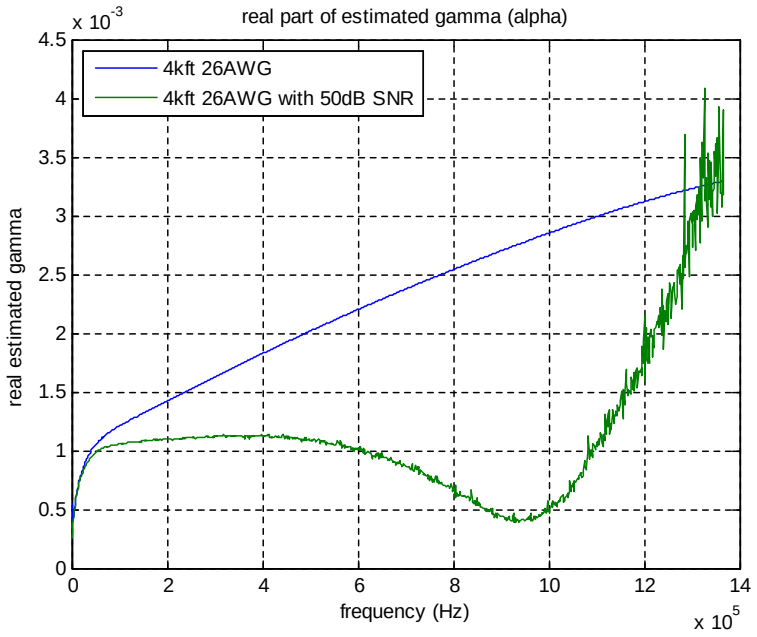

Figure 39: Real part of estimated propagation, 50dB SNR of flat white noise

4.0 CONCLUSIONS

This technique is sensitive to both noise and to differences in source impedance. The system must be designed to drastically reduce noise. This could be done via differential measurements taking advantage of the twisted pair noise cancellation, or other noise cancellation techniques, or if the main source of noise is white, the FDR measurement can be done multiple times and averaged together thus reducing the noise. Noise limitations are common for telecom xDSL testing because of the great losses twisted pair transmission line exhibit for frequencies above voice-band frequencies which are 3.4kHz and higher. The frequency 300kHz, which is a commonly used as a gauge to determine the health of a ADSL line, has losses of ~4.41dB per kft for 26AWG. For a 15kft 26AWG line, the loss is >60dB, for equipment located only at one end this loss exceeds 120dB. Another technique that adjusts for noise conditions is stated in [3]. This technique looks as various frequency ranges so for longer loops where 300kHz loss exceeds 120dB or where noise is excessive, the [3] technique uses lower frequencies which have a higher signal to noise ratio.

Another limitation to this technique is slight mismatches in the source impedance to the line impedance renders this technique useless. Using a calibration scheme that clearly measures the source reflection must be done for cases where the test equipment impedance does not match the line impedance.

With those limitations in mind this technique does reduce the effects of the damping making impedance mismatch reflections located far from the test equipment similar in shape and size to impedance mismatch reflections located close to the test equipment. This result is evident when comparing Figure 28 with Figure 29.

APPENDIX

TWISTED-PAIR PRIMARY PARAMETERS

Table 1: 24-Gauge PIC Cable at 70 Degrees F, adapted from Table 3.3 from Chen[2]

Frequency	**R**	**L**	**G**	**C**
(kHz)	**(ohms/Mile)**	**(mH/Mile)**	**(μ-Mho/Mile)**	**(μF/Mile)**
1	277.23	0.9857	0.115	0.083
2	277.28	0.9852	0.210	0.083
3	277.34	0.9848	0.299	0.083
5	277.48	0.9839	0.466	0.083
7	277.66	0.9829	0.625	0.083
10	277.96	0.9816	0.853	0.083
15	278.58	0.9793	1.213	0.083
20	279.35	0.9770	1.558	0.083
30	281.30	0.9723	2.217	0.083
50	286.82	0.9577	3.458	0.083
70	294.29	0.9464	4.634	0.083
100	308.41	0.9347	6.320	0.083
150	337.22	0.9204	8.993	0.083
200	369.03	0.9087	11.550	0.083
300	431.55	0.8885	16.436	0.083
500	541.69	0.8570	25.633	0.083
700	632.08	0.8350	34.351	0.083
1000	746.04	0.8146	46.849	0.083

Table 2: 26-Gauge PIC Cable at 70 Degrees F, adapted from Table 3.4 from Chen[2]

Frequency	**R**	**L**	**G**	**C**
(kHz)	**(ohms/Mile)**	**(mH/Mile)**	**(μ-Mho/Mile)**	**(μF/Mile)**
1	440.79	0.9858	0.115	0.083
2	440.83	0.9854	0.210	0.083
3	440.88	0.9850	0.299	0.083
5	441.01	0.9843	0.466	0.083
7	441.15	0.9836	0.625	0.083
10	441.39	0.9825	0.853	0.083
15	441.87	0.9907	1.213	0.083
20	442.45	0.9789	1.558	0.083
30	443.88	0.9753	2.217	0.083
50	447.81	0.9660	3.458	0.083
70	453.09	0.9546	4.634	0.083
100	463.39	0.9432	6.320	0.083
150	485.80	0.9306	8.993	0.083
200	513.04	0.9212	11.550	0.083
300	575.17	0.9062	16.436	0.083
500	699.61	0.8816	25.633	0.083
700	812.95	0.8614	34.351	0.083
1000	956.65	0.8381	46.849	0.083

BIBLIOGRAPHY

[1] Starr, Thomas, Cioffi, John M., Silverman, Peter J., Understanding Digital Subscriber Line Technology, Prentice Hall PTR, 1999

[2] Chen, Dr. Walter Y., DSL: Simulation Techniques and Standards Development for Digital Subscriber Line Systems, Macmillan Technical Publishing, 1998

[3] US Patent #6687289, "Method for measuring the attenuation in digital transmission lines", Feb. 3, 2004

[4] Dodds, David E., "Single-ended FDR to Locate and Specifically Identify DSL loop Impairments", IEEE Comm. Soc. ICC 2007 proceedings, pp. 6413-6418

[5] Dodds, David E., Shafique, Muhammad, Celaya, Bernardo, "TDR and FDR identification of bad splices in telephone cables", IEEE CCECE/CCGEI, proceedings May 2006, pp. 838-841

[6] Southworth, George C., Principles and Applications of Waveguide Transmission, D. Van Nostrand Company, Inc. 1950

[7] Tsai, Peijung, Lo, Chet, Chung Chung, You, Furse, Cynthia, "Mixed-Signal Reflectometer for Location of Faults on Aging Wiring", IEEE Sensors Journal, Vol. 5, No. 6, December 2005, pp. 1479-1482

[8] Thomas, Steve, "Antenna System Measurements using Frequency Domain Reflectometry vs Time Domain Reflectometry", Systems Readiness Technology Conference, IEEE, 18-21 Sept. 2006, pp. 230-236

[9] Buccella, C., Feliziani, M., Manzi, G., "Accurate detection of low entity cable faults by wavelet transform", Electromagnetic Compatibility, 2004, EMC 2004, Internation Symposium, Vol. 3, 9-13 Aug. 2004, pp. 936-941